universität wien

MASTERARBEIT / MASTER'S THESIS

Titel der Masterarbeit / Title of the Master's Thesis

„Investigation of Neurite Outgrowth of DRG Neurons upon Inflammatory Stimuli“

verfasst von / submitted by

Verena Hofer, BSc

angestrebter akademischer Grad / in partial fulfilment of the requirements for the degree of

Magistra pharmaciae (Mag.pharm.)

Wien, 2023 / Vienna 2023

Studienkennzahl lt. Studienblatt / degree programme code as it appears on the student record sheet:	UA 066 605
Studienrichtung lt. Studienblatt / degree programme as it appears on the student record sheet:	Masterstudium Pharmazie
Betreut von / Supervisor:	Univ.-Prof. Manuela Schmidt, Ph.D.

Table of contents

List of abbreviations

ASIC ..... Acid-sensing ion channels
BDNF ..... Brain-derived neurotrophic factor
BSA ..... Bovine serum albumin
CNN ..... Convolutional neural network
CNS ..... Central nervous system
COC ..... Cyclic olefin co-polymer
CTR ..... Control
DIV ..... Days in vitro
DMEM ..... Dulbecco's Modified Eagle Medium
DRG ..... Dorsal root ganglion
GABA ..... Gamma-aminobutyric acid
HS ..... Horse serum
IASP ..... International Association for the Study of Pain
IL ..... Interleukin
IVD ..... Intervertebral disk
NGF ..... Nerve growth factor
NSAID ..... Non-steroidal anti-inflammatory drug
NT ..... Neurotrophin
PBS ..... Phosphate buffered saline
PDL ..... Poly-D-lysine
PDMS ..... Polydimethylsiloxane
PGB ..... Pregabalin
PNS ..... Peripheral nervous system
ROI ..... Region of interest
SFN ..... Small fiber neuropathy
SNI ..... Spared nerve injury
TNF ..... Tumor necrosis factor
Trk ..... Tyrosine receptor kinase
TRPV-1 ..... Transient receptor potential cation channel subfamily V member 1
VEGF ..... Vascular endothelial growth factor
VGCC ..... Voltage-gated calcium channel

List of figures

Abstract

Many painful conditions involve an alteration of sensory neurons in the peripheral nervous system (PNS). Some lead to a degeneration while some provoke excessive sprouting of neurites. The mechanism connecting the sensation of pain and inflammation to abnormal neurite outgrowth is complex and remains unclear. This thesis investigates the effect of the pro-inflammatory cytokine tumor necrosis factor (TNF), which is known to be involved in many inflammation-connected pain states and pregabalin (PGB), a common drug for the treatment of neuropathic pain, on the neurite outgrowth of cultured dorsal root ganglia (DRG) neurons from mice. Neurite length is assessed in two ways. While the effect of the stimuli on the whole cell is shown in conventional culture plates, the possibility of solely treating neurites is explored in microfluidic devices. Neurite outgrowth of the same neurons at three different timepoints were imaged as phase contrast images and then were analyzed by a manual tracing method.

The main result is that by treating the whole neuron, TNF and PGB slightly inhibit neurite outgrowth compared to the control neurons. However, the neurites treated in microfluidic devices are not differentiable in their neurite length from control devices.

This study has several limitations, including a low number of biological replicates, disadvantages of the chosen analysis method and differences in experimental design.

In conclusion, this outcome presents an interesting effect of the stimuli on sensory neurons, where with future experiments potential new mechanisms of neurite outgrowth connected to painful conditions in the PNS could be revealed.

Zusammenfassung

Veränderungen von sensorischen Neuronen des peripheren Nervensystems (PNS) bringen oft verschiedene Schmerzzustände mit sich. Dabei können Neurite sowohl degenerieren als auch übermäßig sprießen. Der genaue Zusammenhang zwischen Schmerz und Entzündung mit einem veränderten Neuritenwachstum ist komplex und noch immer nicht vollständig geklärt. Daher wird in dieser Arbeit die Wirkung einerseits des pro-inflammatorischen Zytokins Tumornekrosefaktor (TNF), welches nachweislich in Verbindung mit entzündungsbezogenen Schmerzzuständen steht, und andererseits von Pregabalin (PGB), u.a. ein Standardwirkstoff zur Therapie von neuropathischen Schmerzen, auf den Neuriten-Auswuchs von Neuronen der Hinterwurzelganglien von Mäusen untersucht. Dabei wird die Gesamtlänge der Neurite auf zwei verschiedene Arten bestimmt. Während der Effekt der Stimulantien in herkömmlichen Zellkulturplatten auf die ganzen Neuronen wirkt, wird gleichzeitig auch die Möglichkeit ausgetestet, mithilfe eines Mikrofluidsystems ausschließlich die Neurite mit den Stimulantien zu behandeln. Das Neuritenwachstum derselben Zellen wurde über drei Zeitpunkte lang als Phasenkontrastbilder aufgenommen, welche mit einer manuellen Neuriten-Analysemethode ausgemessen wurden. Daraus resultiert eine leichte Inhibierung des Neuriten-Auswuchs durch TNF und PGB im Vergleich zur Kontrollgruppe, wenn das ganze Neuron behandelt wurde. Andererseits, wenn nur die Neurite stimuliert wurden, lag kein Unterschied in der Neuriten-Länge zwischen Behandlung und Kontrolle vor. Diese Studie unterliegt einigen Limitationen, welche eine geringe Anzahl an biologischen Replikaten, Nachteile der ausgewählten Analysemethode und Unterschiede im experimentellen Design beinhalten. Zusammenfassend geben die Ergebnisse einen potenziell interessanten Effekt auf sensorische Neuronen wieder, welcher mithilfe von fortführenden Experimenten zukünftig zur Entdeckung von neuen Mechanismen von Neuritenwachstum in Verbindung mit Schmerzzuständen im PNS führen könnte.

Graphical abstract

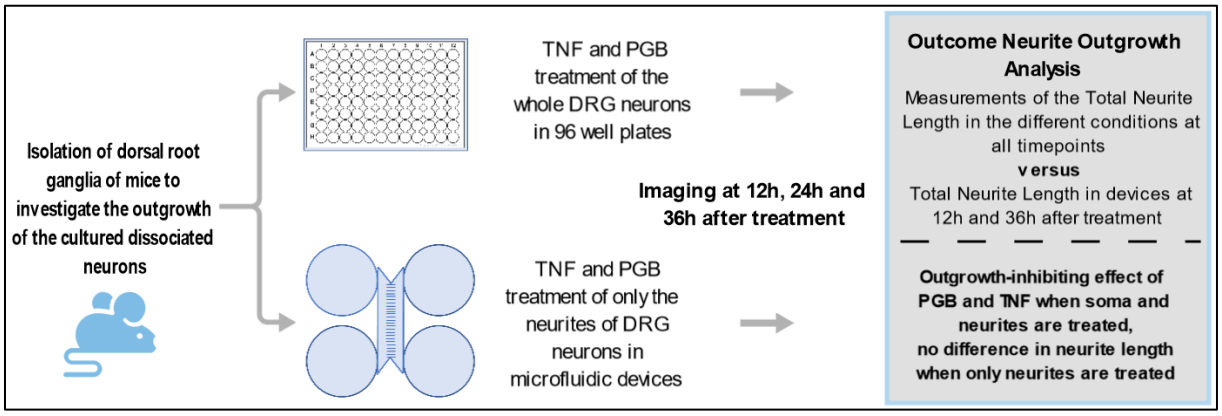

Figure 1: Graphical abstract

1 Introduction

1.1 Pain and the physiology of pain

1.1.1 Acute versus chronic pain and its problems

The International Association for the Study of Pain (IASP) defines pain as the following:

“An unpleasant sensory and emotional experience associated with, or resembling that associated with, actual or potential tissue damage” (Raja et al., 2020).

As acute pain acts as an unpleasant sensation in response to injuries or infections and therefore signals the organism to avoid further damage and starts the healing process, it plays a crucial role in the survival of an organism. On the contrary, as chronic pain lacks most of these functions essential for survival, it does not have a physiological purpose anymore. (Bourinet et al., 2014; Cohen et al., 2021).

With a prevalence of 11 - 40%, chronic pain is a problem, which is affecting a relatively high percentage of the world population. Beyond being an “unpleasant sensory and emotional experience, …” (Raja et al., 2020), chronic pain also is accompanied by psychological, biological and social symptoms, e.g. psychological distress, sleep problems, depression,… (Cohen et al., 2021).

Additionally, around 1/5 of patients affected by chronic neuropathic pain are being insufficiently treated for their condition. Therefore, well-tolerated and more effective

treatment options for chronic pain ailments are needed. Although chronic neuropathic pain is a quite common condition, there are several reasons why its treatment is so problematic. Even though new methods and targets are being tested, they often vary in involved risks and effectiveness for the patients. Especially, pharmacological therapy, like NSAIDs and opioids, show limited effects (Berger et al., 2021). As for opioids, a long-term treatment increases the risk for opioid use disorder, which involves higher morbidity and mortality rates (Malik et al., 2020).

Thus, chronic pain and its treatment, still involve a lot of challenges and pain research represents a very important area to find new therapy options and solutions to treat these painful conditions.

1.1.2 Physiology of pain and nociception

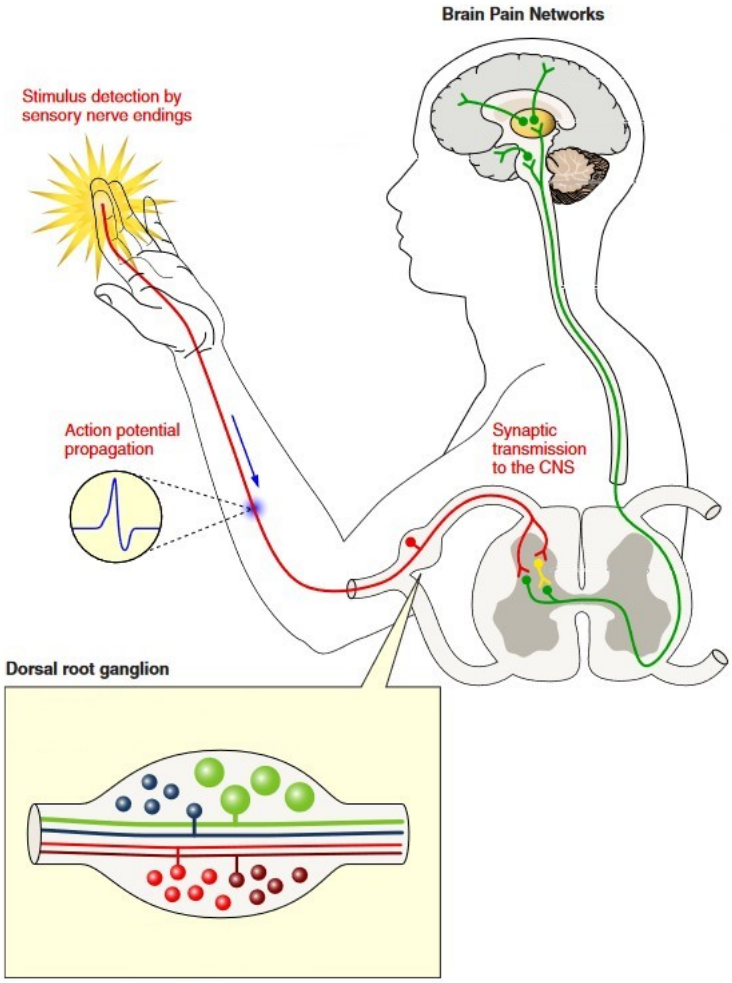

Figure 2: Pain signaling pathway, (adapted from Bourinet et al., 2014)
After the detection of a stimulus in the nerve endings, the signal gets propagated as action potentials through the DRG, spinal cord and into the central nervous system. In the dorsal root ganglia, cell bodies of sensory neurons are located, which also include the cell bodies of nociceptors.

The sensation of pain starts by a noxious, a chemical or mechanical stimulus, which gets detected by nociceptors, a subgroup of peripheral nerve fibers, in internal organs and skin (Figure 2).

The dorsal root ganglia (DRG) contain the soma of these mentioned neurons along with other sensory neurons. Afferent neurons consist of two branches: one presents the connection to the peripheral nervous system and the other branch connects to the spinal cord and ultimately to the central nervous system (CNS). This gives them a pseudo unipolar morphology. Only when the intensity of a noxious stimulus is high enough to pass a threshold, nociceptors are activated and action potentials get propagated along the fibers to the spinal cord and transmissioned by synapses to the CNS. Sensory neurons, whose cell bodies are located in the DRG, can be divided in many sensory fiber subtypes.

There are two classes of nociceptors. The first class consists of medium diameter afferent fibers (Aδ), which are myelinated and therefore propagate acute pain very fast. Thus, the sensation of pain is easy to locate. The second class of nociceptors consist of afferent “C” fibers, which are small diameter and not myelinated, thus propagating signals more slowly. Hence, the origin of the signal cannot be localized clearly and therefore is called “slow” pain (Basbaum et al., 2009; Bourinet et al., 2014).

1.2 Neurite outgrowth in the context of pain

In contrary to most acute pain, chronic pain is connected to changes in peripheral and central sensitization and other morphological and pathophysiological damages. Moreover, chronic pain is associated with developing new neural connections and certain pathological brain modifications (Cohen et al., 2021).

As this thesis aims to investigate the outgrowth of DRG neurons in vitro in two ways, one is the stimulation of the entire cell with TNF and pregabalin, while the other perspective is the isolated stimulation of neurites only, it is important to state, that the altering of neurons is part of many pathological conditions in humans. Those pathologies are associated with influencing the outgrowth of neurites, some promote sprouting and deeper innervation, while other conditions lead to denervation.

1.2.1 Development of the sensory system

To investigate the abnormal neurite outgrowth in the context of diseases, it is also important to understand the physiological development and mechanisms of axonal growth in the PNS.

In short, the development of the nervous system starts by the formation of neurons out of neural stem cells and the initiation of axonal outgrowth. This also involves the development of the connection of the PNS with the CNS. Neurites start to form by growing temporarily short axonal processes out of the soma of the neuron. That is followed by the formation of a mature growth cone, which then follows a defined growth direction. As DRG neurons are of the pseudo unipolar type, both the formation of an axon growing into the spinal cord to connect to the CNS and a projection of an axon into peripheral regions to innervate muscles, skin and organs develops. Each step of the formation of the PNS is accompanied by a complex interaction of signal molecules secreted by the surrounding tissue. They either encourage or repel neurite growth into their direction helping the formation of the intricate sensory nervous system. The molecules aiding the development of axons are the netrins, slits, semaphorins and ephrins. They withhold either outgrowth-stimulating or outgrowth-inhibiting effects which guide the neurons in their development to properly innervate their dedicated tissue (Holt et al., 2021; Koncina et al., 2007).

The development of the nervous system in embryos presents itself as a very complex matter with endless mechanisms allowing the correct peripheral neurons to innervate into their dedicated target tissue. Yet, when neurons are injured in a fully developed organism also other mechanisms come to play, as it involves the question on how and to what extend neurons regenerate and regain their function.

1.2.2 Nerve injury and regeneration

Injuries of the peripheral nervous system (PNS) frequently result in pain, which, even though the initial injury is already resolved, stay in a prolonged state of pain. Part of this development is neuroinflammation, a stationary inflammation happening in the PNS and CNS responding to injury, which is technically responsible for healing and regeneration, however also evidently involved in turning into a maladaptive process resulting in chronic pain (Ji et al., 2016; Sommer et al., 2018).

After a peripheral nerve is damaged, it has limited possibilities to regenerate and reconnect with its intended tissue. Nerve fibers are able to regrow into their previous tissue. If the regrowth is blocked, there is also the ability of undamaged, surrounding nerve fibers to reinnervate the affected tissue by collateral sprouting (Griffin et al., 2010). Peripheral nerve fiber regeneration starts quickly after the injury occurred. It depends on molecular changes in the affected tissue and in DRG somas to first commence Wallerian degeneration and then to form growth cones to start the actual regeneration. TNF also seems to play an influential role in peripheral nerve regeneration. There is evidence that etanercept, a TNF-antagonist, given its administration in early stages after nerve injury, could speed up the process of axonal regeneration. (Kato et al., 2010).

The connection between nerve regeneration after a physical trauma and chronic pain has not been discussed often in existing literature. It is still unclear, if neuronal reinnervation and therefore the reorganization of neurons after a trauma is causing neuropathic pain or develops because of it. However, new evidence from a SNI (spared nerve injury) mouse model suggests, that after nerve injury reinnervation-induced neuropathic pain can evolve. This presents a new form of neuropathic pain with a rather late development after reinnervation linked with miswiring, malfunctioned nociceptors and structural plasticity (Gangadharan et al., 2022).

1.2.3 Other diseases connected to structurally altering sensory neurons

a. Cancer

Nerves and cancer are connected in their interaction quite closely. It is known that remodeling and aberrant plasticity of sensory neurons can lead to cancer-induced pain (Park et al., 2021). In cancer-induced bone pain, the outgrowth and sprouting of sensory neurons is part of its pathomechanism, leading patients to feel pain when cancer cells build metastasis in the bones (Mantyh et al., 2010). Another trigger for chronic pain in the context of cancer with a nerve-altering mechanism is nerve damage. Chemotherapy-evoked neuropathic pain is induced by different classes of antimitotic drugs, e.g. vinca alcaloids and taxanes, by evoking a degeneration of the terminal arbors of primary afferent sensory neurons in the skin (Xiao & Bennett, 2008). Furthermore, levels of TNF and IL-1β (Interleukin 1 beta), inflammatory cytokines, are elevated in lumbar DRGs during paclitaxel treatment (E. Kim et al., 2019).

b. Endometriosis

The pathomechanism of endometriosis involves hyperinnervation and an elevated density of nerve fibers in ectopic endometrium tissue, which leads to endometriosis-associated pain (Yan et al., 2017). Studies reveal, that peritoneal fluid of endometriosis patients stimulates the growth of neurites in sensory ganglia, due to an overexpression of NGF, which plays an important role in the outgrowth of sensory neurons (Arnold et al., 2012).

c. Low back pain

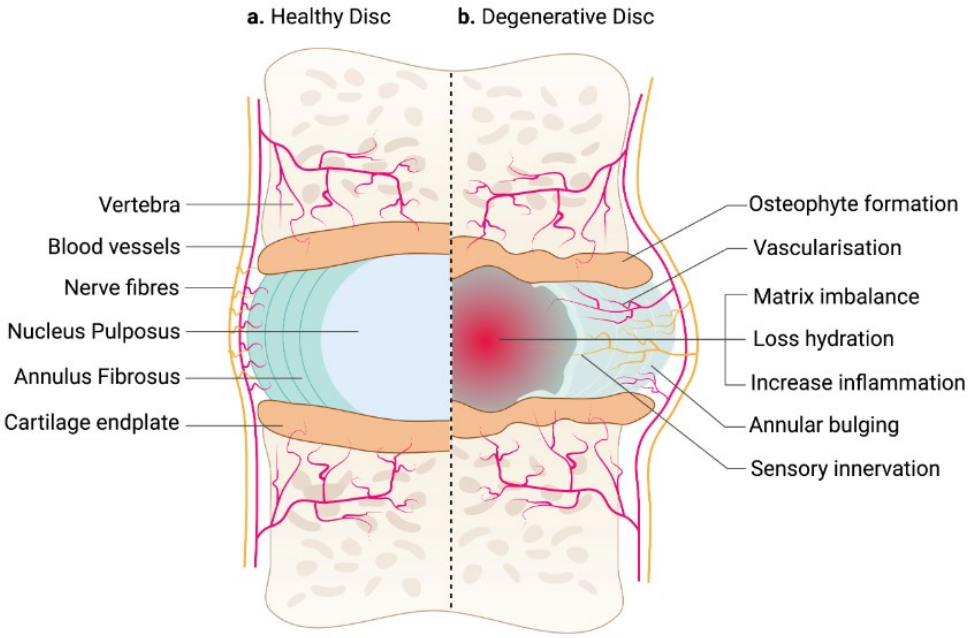

Figure 3: Healthy versus degenerated disc (Mohd Isa et al., 2023)
The image on the right shows a degenerated disc with excessive ingrowth of neurons potentially causing pain compared to a healthy intervertebral disc as seen on the left.

The primary area causing low back pain are degenerated intervertebral discs (IVDs) (Ogon et al., 2015). There is a connection between patients experiencing back pain and degenerated IVDs with ingrowth of substance-P-expressing nerves (Figure 3). Mentioned neo-innervation is strongest in IVD levels where pain is located (Freemont et al., 1997; Mohd Isa et al., 2023). It has been shown, that in degenerated IVDs heightened levels of IL-8, TNF, TGF-β, VEGF (vascular endothelial growth factor) and NGF can be found. These proinflammatory cytokines and neurotrophic factors

are currently believed to greatly influence the pathomechanism, especially the neo-innervation, of the condition (Lee et al., 2009).

d. Small fiber neuropathy

Small fiber neuropathy (SFN) is a condition involving unmyelinated C-fibers and myelinated Aδ-fibers, where distal terminations of the involved fibers degenerate and denervate. The denervation reduces skin innervation and leads along with other factors to SFN pain (Hoeijmakers et al., 2012). Its clinical characteristic is a burning painful sensation in the feet and sometimes in the hands. Associated diseases include diabetes mellitus, hypothyroidism or due to genetic predisposition (Sommer et al., 2018). In studies investigating the interaction of keratinocytes and fibroblasts with small nerve fiber endings and cytokine gene expression profiles in patients, inflammatory cytokines, e.g., IL-6 and IL-8, were found to be higher expressed than in their controls, which could play a role in the nociceptor degeneration. Although higher concentrations of cytokines can be found, there is still no proven connection of SFN pain and cytokine expression levels (Kreß et al., 2021; Sommer et al., 2018).

By studying the pathomechanism of each of these diseases it becomes evident, that often a transformation of neurons is involved. Furthermore, both an outgrowth-inhibiting effect and an outgrowth-stimulating effect of stimuli can be part of the development of a painful condition, therefore deciphering stimuli having these effects could play an important role in decoding the mechanism of pain and in the future in developing potential new targets for pain treatment.

1.3 Inflammation, cytokines, stimuli and other outgrowth-influencing factors

1.3.1 Inflammation

The five cardinal features of inflammation are swelling (tumor), redness (rubor), loss of function (function laesa), elevated temperature (calor) and pain (dolor). These acute reactions that belong to the characteristics of inflammation play a very important protective role in ultimately resolving and healing from the initial cause, as they are one factor in preventing the organism to avoid harmful stimuli and protect harmed tissue. Inflammation involves a lot of different cells and mediators including immune cells and inflammatory cytokines (Ji et al., 2016; Matsuda et al., 2019). As acute pain is included in the cardinal signs of inflammation, evidence suggests that

most inflammatory mediators are able to cause pain by exerting their effects on receptors of nociceptors of primary sensory neurons (Ji et al., 2014, 2016).
After a peripheral injury, as part of the inflammatory process, cytokines such as TNF and IL-1β stimulate fibroblasts and keratinocytes, which then secrete NGF. The ongoing signal cascade with many more players involved, then ultimately leads to the sensitization of nociceptors and hyperalgesia (Shu & Mendell, 1999).

1.3.2 Cytokines

Specifically influencing the interaction from cell to cell, cytokines play an important role of mediating and communicating between cells. They are secreted proteins with a multitude of effects and are released by cells to operate their effect on themselves, neighboring cells and rarely even faraway cells. Often, one cytokine can have effects on many different cells and different types of cells can release the same cytokine. The release of cytokines is often part of a cascade, where released cytokines stimulate cells to secrete more cytokines to continue its effects. Proinflammatory cytokines, involved in further promoting inflammatory responses, are mainly secreted by activated macrophages and evidently play a role in the mechanism of action of pathological pain (J.-M. Zhang & An, 2007). Anti-inflammatory cytokines seem to also play an important function in chronic pain as there are several studies showing an analgesic effect (Sommer et al., 2018).

1.3.3 Tumor necrosis factor

The pro-inflammatory cytokine tumor necrosis factor (TNF) is part of the initial inflammatory response, where its release has algesic and inflammatory effects. Physiologically, the hyperalgesia occurring during an acute inflammation is partly a result of inflammatory cytokines, such as TNF (Junger & Sorkin, 2000). However, also pathophysiologically, evidence suggests, that the release of TNF is linked to the development and its maintenance of neuropathic pain. TNF is released by cells of different kinds, such as immune cells like macrophages, but also astrocytes, microglia, Schwann cells, fibroblasts and endothelial cells (Wagner & Myers, 1996).
The effects of TNF on the regulation of pain signaling can be divided in short and long acting. Short acting, there is evidence that it modulates ion channels in their activity, like for example the increase of the expression of Nav1.7, which can be found in the nociceptive fibers Aδ and C, or rapidly boosting acid-sensing ion channels

(ASIC's) electrophysiological activity, which leads to peripheral sensitization and evokes pain in behavioral studies. Long acting, TNF is capable of changing the expression of different other mediators and signaling proteins involved in inflammatory pathways (de Macedo et al., 2019; S. Wei et al., 2021).

On behalf the effects of TNF on neurite outgrowth, it is assumed to play a role in the neo-innervations of degenerated IVDs, but also in modulating nerve regeneration after nerve injury (Kato et al., 2010; Lee et al., 2009).

The concentration of 100 ng/ml TNF for the experiments of this study goes along with previous experiments, where this concentration of TNF was used for calcium imaging with DRG neurons (Segelcke et al., 2021).

1.3.4 Pregabalin

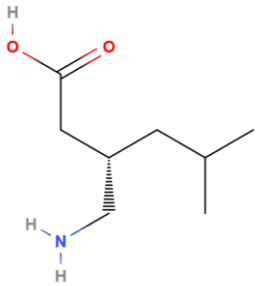

Figure 4: Pregabalin 2D-structure
(S)-3-(Aminomethyl)-5-methylhexanoic acid

The small molecule Pregabalin (PGB) is classified together with Gabapentin as "gabapentinoids", which are drugs originally developed to be structurally similar to GABA (gamma-aminobutyric acid), an inhibitory neurotransmitter, to act as an anticonvulsant. However, neither Pregabalin nor Gabapentin act as GABA mimetic and the ion channels $GABA_A$ or $GABA_B$ do not get activated by them. Instead, these gabapentinoids show a selective and potent binding activity to α2δ-1 and α2δ-2 subunits, two out of the overall four subunits of voltage-gated calcium channels (VGCCs) (Li et al., 2011).

As a therapeutic, PGB is currently used for the treatment of epilepsy (as add-on therapy), neuropathic pain and generalized anxiety disorder. Regarding the mechanism of action, there is mixed evidence. Gabapentinoids possibly could reduce presynaptic cellular calcium influx due to VGCC binding, which could lead to a reduction of neuronal calcium current and therefore less excitatory neurotransmitters, who are re-

sponsible for aberrant hyperexcitability in the different pathologies (Calandre et al., 2016).

In terms of the mechanism for the treatment of neuropathic pain, studies with rodent nerve injury models show, that α2δ-1 is higher expressed in certain tissue, especially in DRG and primary afferent nerve terminals, which leads to allodynia, the excessive sensitivity to normal touch (Luo et al., 2001). PGB then seems to have an anti-allodynic effect by hindering the trafficking of this subunit from the DRGs to presynaptic terminals of the spinal cord, which also leads to reduced amounts of neurotransmitter being released (Bauer et al., 2009).

Considering PGB influencing neurite outgrowth of DRG neurons, PGB could improve axon regeneration after spinal cord injury and could lessen neurite shortening effects after chemotherapy treatment (Martínez et al., 2021; Tedeschi et al., 2016). As one previous study explored the effects of pregabalin on the outgrowth of DRG neurons, 250 µM as the concentration for these experiments was chosen accordingly (Tedeschi et al., 2016).

1.3.5 NGF as outgrowth-influencing factor

Nerve growth factor (NGF), along with neurotrophin NT-3, NT-4 and brain-derived neurotrophic factor (BDNF), belong to the protein family of neurotrophins. NGF and the other neurotrophins bind to the tyrosine receptor kinase (Trk) A, B or C and to the p75 receptor, which is a part of the tumor necrosis receptor superfamily (Chao, 2003).

Neurotrophins inherit important functions in the development, growth and specification of the PNS before birth. After birth, they play a role in neuronal regeneration, proliferation, maintenance, survival and in the formation of pain, e.g. NGF shows an overexpression in different human pain conditions (Malfait et al., 2020).

Evidence suggests that there is also a relation between TRPV-1 (transient receptor potential cation channel subfamily V member 1), which is involved in nociception, and NGF, where sensory neurons show a higher response to TRPV-1 agonist capsaicin when NGF is also present (Shu & Mendell, 1999).

Therapeutically, NGF is used to treat various diseases. Taking opportunity of its ability to induce neurite outgrowth, it is applied as a therapeutic in peripheral nerve injury, but unfortunately facilitates neuropathic pain at the same time. Therefore, new thera-

peutics possibly without these side effects, such as Maresin 1, are being proposed (J. Wei et al., 2022).

Due to NGFs and other neurotrophins survival and proliferation promoting functions it is a staple in use for culturing DRG neurons. Hence, it was also used for all experiment cultures during this thesis.

1.4 Compartmentalized chambers

In typical in vitro cultures of neurons performed in conventional culture dishes, a stimuli treatment will always lead to a response of cell somas and their neurites. It is also interesting to investigate the response of isolated axons to certain stimuli and its possible effects on the whole neuron without treating the cell bodies themselves (Atmaramani et al., 2021). Therefore, compartmentalized cultures were developed. To separate neuron cell bodies from their neurites, two types of compartmentalized systems for neuronal cultures are most commonly used, the earlier developed “Campenot chamber” and then later microfluidic devices. Usage of devices like these give a possibility for separation and exclusive treatment of either somata or neurites (Wang et al., 2020).

1.4.1 Campenot chambers

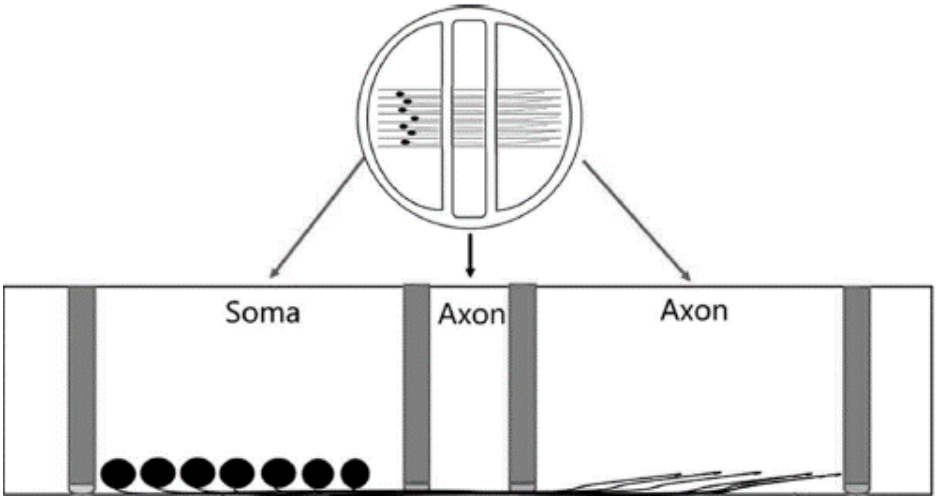

Figure 5: Campenot chambers (adapted from Wang et al., 2020)
Separated by the Teflon divider, Campenot chambers allow a separation of soma and axons of neurons, where each compartment can be treated with different stimuli.

The “Campenot chamber” was first described in 1977 by Robert B. Campenot. It consists of a 35mm petri dish with a coverslip coated with a collagen film. Into this collagen layer 20 parallel channels, with a spacing of 200 µm in between, were scraped with needles. On top of the coverslips a “Teflon divider” was latched on with silicone

grease. The Teflon divider had the purpose of separating the chamber into three compartments. Campenot described, that due to the parallel scratches in the collagen, neurite outgrowth tended to follow the channels instead of growing in an unorganized way. In this chamber setup maintaining different fluid-levels were possible, still allowing neurites to cross between the chamber boundaries (Campenot, 1977, 1979). In fact, the silicone grease presents itself as a stable barrier between the chambers, as the different fluid-levels stay intact for up to a few days (Campenot, 1979).

With this described technique, Campenot did experiments with mostly neurotrophic factors. The ability of NGF to increase neurite outgrowth locally was discovered (Millet & Gillette, 2012). Generally only peripheral neurons work with this method, because of the rather long distance between compartments, where a long extension of neurites is required (Campenot, 1977). Other than the studies on neurotrophic factors, (Campenot, 1977, 1979, 1982, 1994), Campenot chambers have also been used for various studies for example on topics of lipid metabolism and transport (Karten et al., 2005) or viral transport mechanism analysis (Kramer et al., 2012).

Because experiments with Campenot chambers are limited to peripheral neurons and neurons must be strong enough to be able to extend across the vacuum-grease barrier, this method is unavailable for neurons of the CNS. Another limitation comes with the assembly of the chambers, which can bring up difficulties with leakage between the compartments and therefore experience from experimenters is required (Millet & Gillette, 2012; Palumbo et al., 2021).

1.4.2 Microfluidic devices

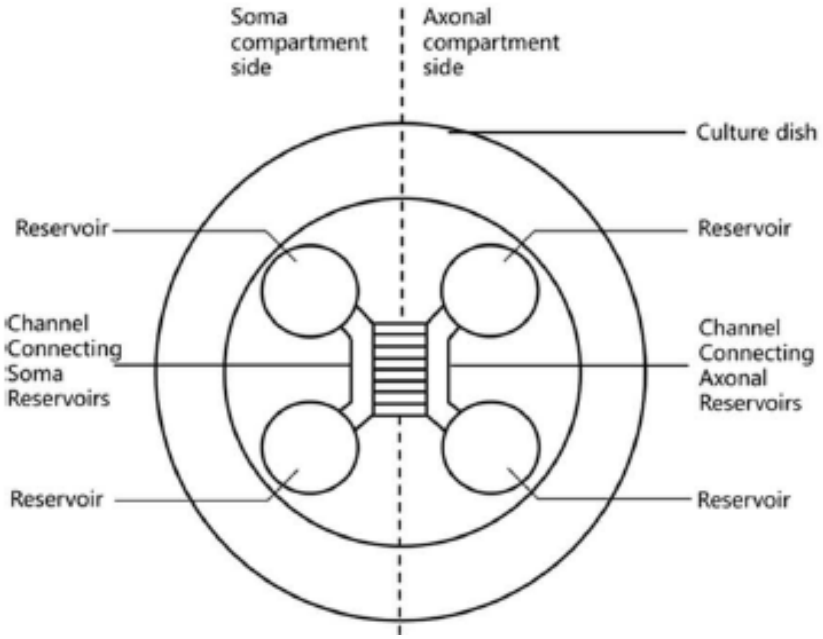

Figure 6: Microfluidic device (adapted from Wang et al., 2020)
A microfluidic device consists of a somal and axonal compartment side, which are connected by microgrooves. Each side can be accessed by two reservoirs/wells. There media can be added, which will be flooded through the main channels and through the microgrooves. Neurons are seeded into the somal compartment side into the main channel, where they can grow neurites through the microgrooves into the main channel of the axonal compartment.

With microfluidic compartmentalized devices a more modern method of in vitro models for culturing neurons and investigating their morphology and function were developed. They differ to Campenot Chambers especially in regard to their material and their way of production and fabrication. The most commonly used material for microfluidic devices is Polydimethylsiloxane (PDMS). They are commonly manufactured by researchers in their own laboratories or also available for purchase (Millet & Gillette, 2012). Recently, pre-assembled chips made of cyclic olefin co-polymer (COC) manufactured by injection molding were introduced. The manufacturer states that their chips have the advantage of not having to be assembled like PDMS devices onto glass slides first by plasma or non-plasma bonding and less hydrophobicity of COC than PDMS. (Mukhopadhyay, 2007; Paranjape et al., 2019; Nagendran et al., 2018). For experiments with microfluidic devices in this thesis the mentioned pre-assembled “XonaChips” made of COC were used.

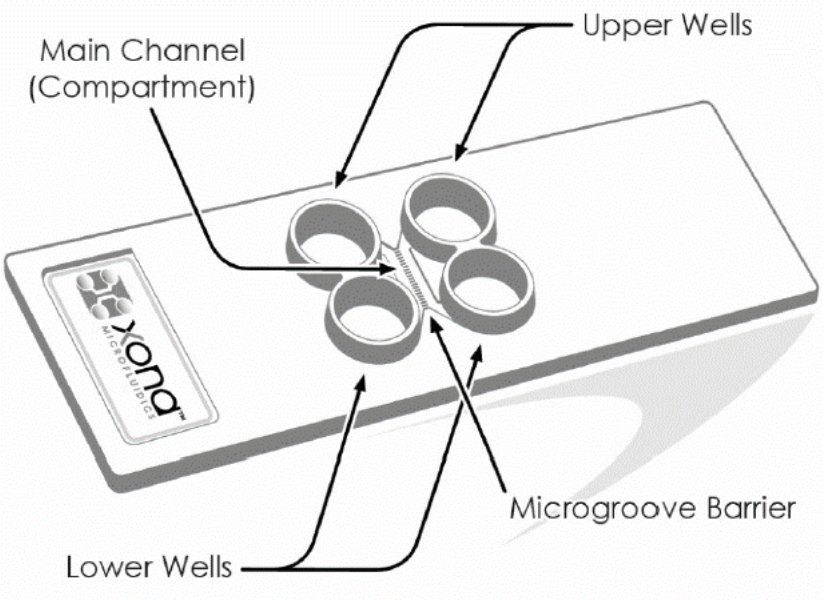

Figure 7: XonaChip (Xona Microfluidics, Inc, 2020)
The microfluidic chips are microfluidic devices, which are integrated in an object slide. In contrast to conventional microfluidic devices, chips are pre-assembled and consist of COC.

There are different designs to microfluidic devices. Generally, they consist of two or three compartments which are connected by microgrooves of different lengths. Neurons are seeded into the somal compartment, where only their neurites can grow through to the axonal compartment. Four wells in each device give access to the compartments and act as medium reservoirs. PDMS devices need to be bonded to a glass slide either by plasma-bonding or non-plasma bonding, whereas chips can be used right away.

Microfluidic isolation is established by a difference in medium volume between both compartments, meaning that a higher liquid volume in one compartment will prevent liquid in the lower volume compartment from mixing with the other compartment liquid due to the opposing micro flux (Clark et al., 2018). The manufacturer states in the protocol for the chips that if properly established, it can be maintained for up to 24h (Nagendran et al., 2018; Paranjape et al., 2019; Xona Microfluidics, Inc, 2020).

Many papers with experiments on DRG neurons in microfluidic devices build up a “neurotrophic gradient” in order to, next to the micro flux, encourage neurite outgrowth through the microgrooves into the opposite compartment. Neurotrophic gradient in that sense means that different concentrations are established during the time the neurons are cultured in the devices. In the first DIV’s a high concentration of growth factors are added to both compartments, the following DIV’s the concentration of growth factors gradually get lowered in the somal compartment, while in axonal

compartments the concentration is kept high (Atmaramani et al., 2021; Clark et al., 2018; Tsantoulas et al., 2013). However, neurons also find their way through the microgrooves with a stable concentration of one or several neurotrophins (Jocher et al., 2018; Vysokov et al., 2019). Therefore, for experiments in this thesis, a stable concentration of NGF was added to the devices.

1.4.3 Opportunities of compartmentalized neuronal cultures

Altogether, these microfluidic devices bring many opportunities for deepening knowledge about the function of neurons and their neurites in vitro especially combined with other methods. Next to outgrowth analysis of DRG neurons during different conditions, like exerted in this thesis and others, the neurites in the axonal compartments can be separately stimulated and the soma investigated via radiometric calcium imaging and/or patch clamp electrophysiology experiments (Atmaramani et al., 2021; Clark et al., 2018; Jocher et al., 2018; Tsantoulas et al., 2013; Vysokov et al., 2019). Moreover, experiments including co-culturing keratinocytes in one of the compartments with the neurites of DRG growing into the keratinocytes, therefore mimicking a simple model of the skin in vitro, provide a lot of interesting research opportunities (Belamadni et al., 2022; Tsantoulas et al., 2013).

1.5 Aim of work

This project aims to investigate neurite outgrowth upon different stimuli administered to DRG neurons in two different methods. On one hand, DRG neurons cultured on conventional well plates were treated with TNF or PGB and then were left to grow for up to 36h. The total neurite outgrowth 12h, 24h and 36h after treatment was then measured and analyzed. On the other hand, DRG neurons were seeded to special neuronal culturing devices, so-called microfluidic devices, which enable a separation of DRG soma from their neurites. The cell bodies of the sensory neurons stay in the somal compartment of the devices where they were seeded into. Only neurites are able to cross through fine channels (microgrooves) into the other compartment of the devices.

In the second part of the experiments, when neurites arrived in the axonal compartment, they were treated selectively with PGB and TNF. This was ensured by microfluidic isolation, which is established by maintaining different fluid levels in axonal and somal compartment of the microfluidic devices.

This is in contrast to the experiments in well plates, where neurons, cell bodies and neurites were all treated jointly. The microfluidic devices were also imaged for up to 36h after the treatment to find potential differences between only stimulating neurites versus stimulating the whole neurons. This was done by analyzing the total neurite length of both methods.

2 Materials and methods

2.1 Materials

2.1.1 Chemicals, media and reagents

Label	Supplier	Composition
BSA	Sigma	
Calcein-AM	Sigma	4mM stock in DMSO
Collagenase Type IV	Gibco	
DBPS 1X	Gibco	
DMEM/F-12 (1:1) (1X) + GlutaMAX-I	Gibco	
DMEM/F-12 (1:1) (1X) + GlutaMAX-I + serum	Gibco	10% horse serum added
Ethanol	Sigma	
Horse Serum	Gibco	
Laminin	Invitrogen	
MolBio H_2O	Lonza	
Papain	Worthington	
PDL	Sigma	
Pregabalin	Sigma	
rhβ-NGF	R&D	
TNFα	Peprotech	dPBS + 0,1% BSA
XC-PreCoat	Xona Microfluidics	

2.1.2 Materials

Label	Supplier	Description
4 Well Plate Dish	Fisher Scientific	
Tissue Culture Plate 96 Well	Falcon	Flat bottom with low Evaporation Lid
XonaChip 450 µm XC450	Xona Microfluidics	

2.2 Methods

2.2.1 Experimental animals

For the experiments of this thesis, DRG neurons were collected from in-house-bred female mice of the C57BL/6 J strain between 8 and 9 weeks old. According to animal welfare guidelines, all mice were sacrificed by carbon dioxide.

2.2.2 Preparation of the microfluidic chips

XonaChips were prepared in accordance with the manufacturers protocol including some minor alterations (Xona Microfluidics, Inc, 2020). First, three devices were placed into 4-well-plates, leaving one well free, where sterile water is added to minimize medium evaporation in the chips. XC Pre-Coat, consisting of 70% ethanol, was used to precondition the chips. All liquids were added in the same order to minimize the risk of introducing bubbles into the main channels or microgrooves. Additionally, liquids should only be added by pointing the pipet tip to the opposite wall of the entrance to the main channel to avoid the formation of bubbles (Figure 8).

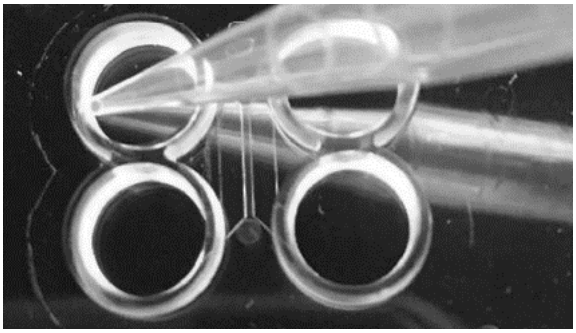

Figure 8: Angle for pipetting liquid into microfluidic chip (adapted from Xona Microfluidics, Inc, 2020)

First the upper left well was filled with liquid, then the solution was allowed to flow through the main channel for 1 min. After liquid was added to the lower left well, during a 5-minute interval, the solution could flow through the microgrooves. Following, the upper right well was filled, and again after 1 min, the last lower right well could be filled up with solution. Another waiting time of 3-5 min was required, before being able to aspirate solution carefully again from the wells. After the preconditioning with Pre-Coat, the chips were washed twice with PBS according to the order described above. Following, the first coating with PDL (1mg/ml) could be added and was incubated for 1,5h. The second coat with laminin (20µg/ml) was added after two rounds of PBS washing steps and once again incubated for 30 min. After aspirating the laminin from the devices and once rinsing the chip with PBS, medium with horse serum

was administered and the chips were placed in the incubator until the neurons were ready to be plated.

2.2.3 DRG culture

DRG of one mouse (for well-plate experiments) or two mice (for devices experiments) were collected in DMEM/F-12 + GlutaMAX-I medium and swiftly moved to be dissociated for 60 min by collagenase in the incubator. The tube was shaken every 15 min to ensure a sufficient dissociation. After the incubation time, the DRG were mechanically triturated with a pipette tip and for 30 min further digested in papain. The cell pellet after centrifugation was mixed with DMEM/F-12 + GlutaMAX-I + 10% horse serum (HS). To separate DRG neurons from other cell debris, a BSA (bovine serum albumin) column step was performed. After centrifugation, the cell pellet was resuspended in the above-mentioned medium with horse serum extended with 100ng/ml of NGF.

2.2.4 Seeding of neurons, treatment and media changes

To seed the neurons in the 96 well plates, 290µl of medium was added to the cell pellet and 9µl of cell suspension was plated into 32 wells. The wells were first coated for 1,5h with PDL (1mg/ml), then washed three times with PBS, and finally coated with Laminin (20µg/ml) for 30 min. After the incubation time, the coating solution was aspirated from the wells. Subsequently the neurons were plated into the coated well plates. For 20 min the neurons were left to adhere to the bottom of the well plate in the incubator, before medium with serum and NGF was added. Finally, the neurons were treated with the different conditions by treating a third of the wells with either 100ng/ml TNF, 250µM PGB or just medium.

Seeding Neurons into the Microfluidic Devices:

First the two cell pellets were resuspended in 15µl of medium with serum and NGF each, then the cell suspensions were mixed and after aspirating the medium from the wells of the chips, 5µl of cell suspension was added to the upper left main channel entrance angling the pipet tip right to the entrance (as shown in figure 9). Another 5µl was added to the lower left channel entrance likewise. After 20 min of incubation time to ensure adherence of the neurons to the main channel, 150µl of medium with serum containing NGF was added simultaneously to both wells of the somal compart-

ment, and then 100µl of the same medium was added at the same time to the bottom wells. The addition of medium in this step was realized simultaneously to avoid flooding the neurons out of the main channel again.

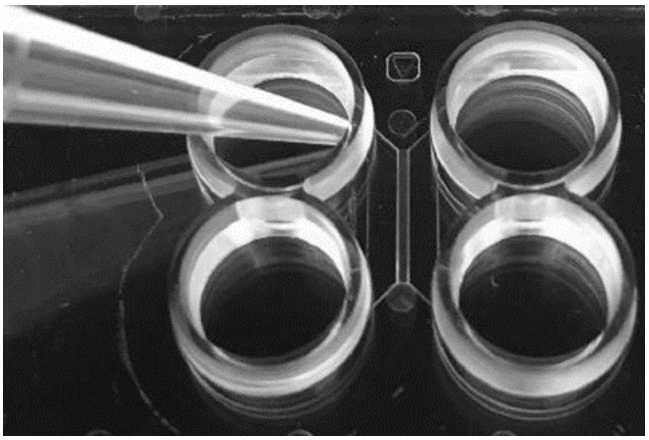

Figure 9: Angle for pipetting cells into microfluidic chips (adapted from Xona Microfluidics, Inc, 2020)

Although the 4-well plate contained extra water, media evaporation still occurred in the devices. Therefore, on DIV 1, 30µl of medium was added to each well, maintaining the microfluidic flux from the somal compartment to the axonal side.
On DIV 2, 48h after seeding the neurons into the devices, the axonal compartment was treated with either 100 ng/ml TNF, 250µM of PGB or plain medium. For this application of stimuli, the entire medium was changed in every device, the stimuli were solved in smaller portions of medium and added to the corresponding axonal compartments.
When devices were kept until DIV 5-10, every second day the medium was changed and the chips were checked daily for evaporation, to add, if needed, 30µl of medium to each well.

2.2.5 Staining with calcein-AM

To stain either the neurons in the well plates or the neurites in the devices, first the Calcein-AM-PBS solution was prepared in a dilution of 1:2000. Then, the old medium was carefully aspirated from the wells/devices and they were washed with PBS. After removing the PBS again, the calcein-solution was added and left to incubate for 15-20 min in the incubator at 37°C before imaging.

2.2.6 Imaging - phase contrast, fluorescence and timelapse

Each 96-well plate outgrowth experiment was imaged 12h, 24h and 36h after treatment. At the first imaging session, 3-5 positions per well were defined in “Multi-Dimensional Acquisition”, so that each image could be observed at every timepoint, enabling the possibility to track neurite growth of the same cells from timepoint to timepoint.

All phase contrast images for analysis were taken on the 20x zoom lens with an exposure time of 10ms, while fluorescent images with the 20x lens needed an exposure time of 3000ms.

The microfluidic devices were imaged similarly to the well plates, with several differences. First, 24 images in total were taken with the 20x lens at every timepoint (12 images per row). Second, due to the difference in the experimental design of the well plate experiments, there were slightly different imaging timepoints. The axonal compartment of each device was treated with each stimulus only 48h after seeding, then was imaged 0h, 12h, 24h and 36h after treatment. At 36h after treatment, a calcein staining of the neurites was performed and imaged.

For a timelapse of the well plates and the devices, the plates were put into environmental control “OKOLAB” with 37°C, 5,0% CO_2, and 50% humidity. Then, positions of interest could be defined and saved in “Multi-Dimensional Acquisition”, where at defined timepoints, the microscope imaged automatically.

2.2.7 Analysis

To analyze the well plate outgrowth experiments five images of all three timepoints per condition and per experiment were selected. Selected images were blinded to avoid bias and then analyzed. The manual analysis of the neurite lengths of the images was performed in Fiji/Image J.

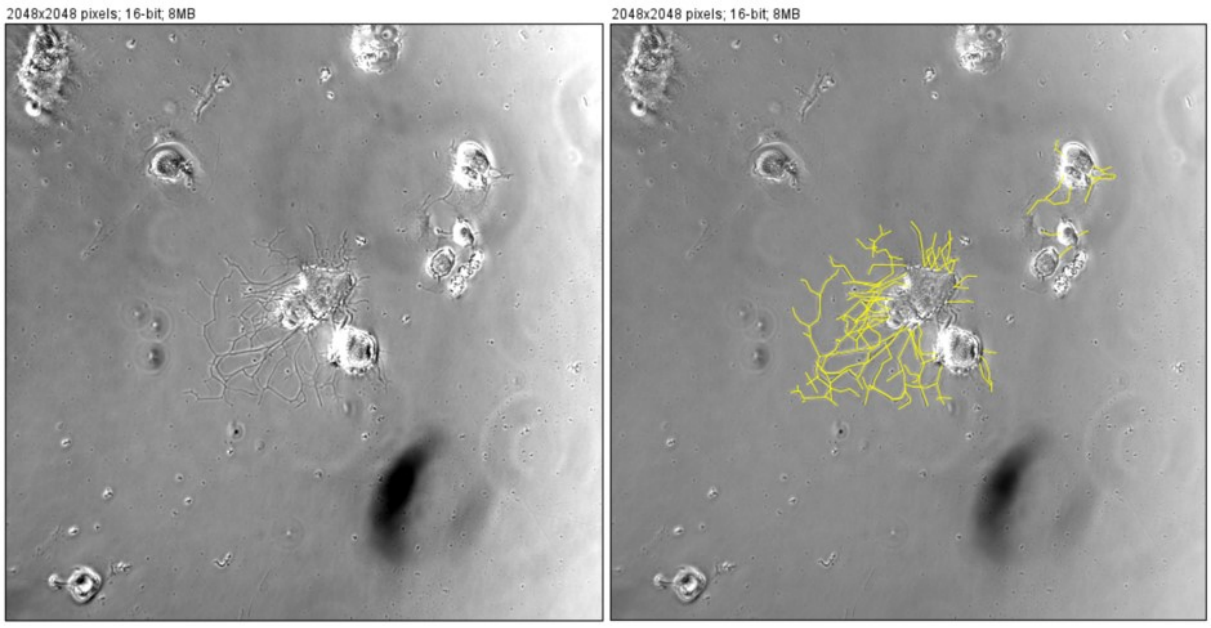

Figure 10: Example for the manual tracing of neurites on well plates
On the left image, neurons are cultured for 36h in medium with TNF, which were traced with the "segmented line" tool in Fiji/Image J on the right. After tracing all the neurites visible, their total length was measured. Additionally, using the "cell counter" tool, cells were counted (not shown in picture).

After setting the scale in Fiji/Image J, cells on each image were counted using the "cell counter" tool. For each image, the total count of cells and the count of cells growing neurites were acquired. Furthermore, as shown in figure 10, each neurite was manually traced with the "segmented line" tool and saved as a ROI (region of interest). Following the tracing, each ROI was measured. The column "length" was then summed to obtain the total length of neurites of one image.

The analysis of the devices was similar. However, no cells needed to be counted, only neurite were analyzed manually lengths from 12h and 36h after treatment (Figure 11). The total length of all 24 images of one device were summed for further calculations.

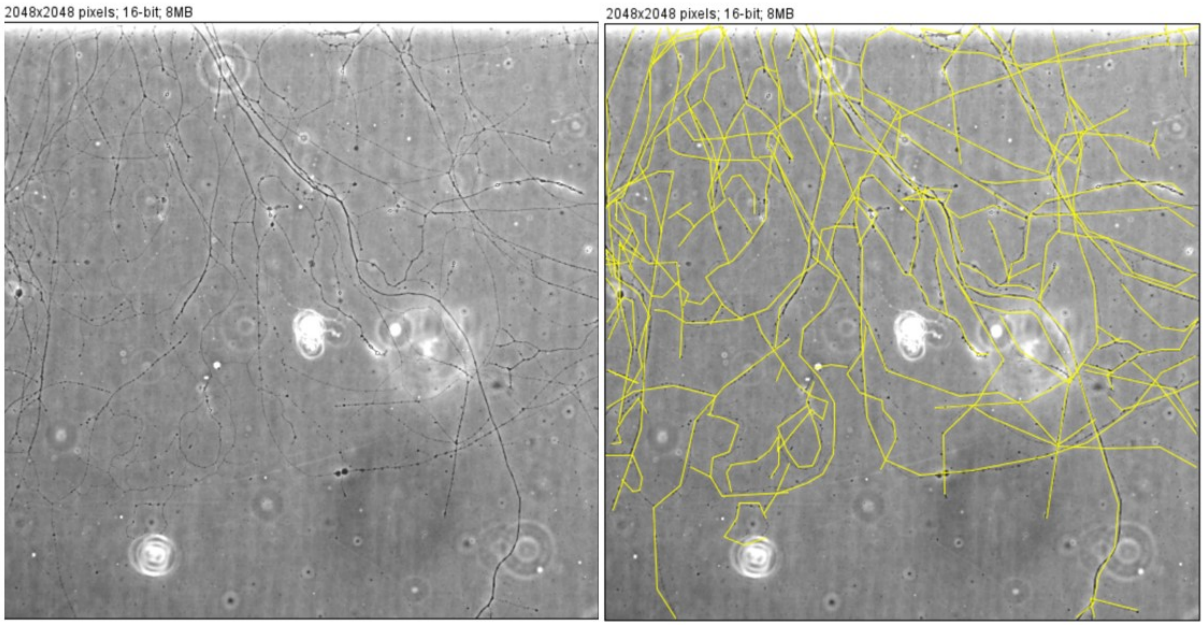

Figure 11: Example for the manual tracing of neurites in microfluidic devices
Before and after image of the exerted tracing method for measuring neurite length of the axonal compartments of the microfluidic devices. Using the “segmented line” tool from Fiji/Image J, each visible neurite was traced and defined as a ROI. For each device of each condition and timepoint 24 images were taken and later analyzed after being blinded regarding their treatment.

3 Results

3.1 Neurite outgrowth on well plates

Experiments in the 96 well plates were repeated four times resulting in four biological replicates. There were 10 wells for each condition per experiment, where five random images per timepoint and condition were chosen to be blinded and then analyzed. Here, individual datapoints are defined as the 20 neurite length values received from the five analyzed images per biological replicate. Additionally, neurons in the images were quantified, here described as the total count of cells and the count of cells growing neurites.

3.1.1 Individual datapoints

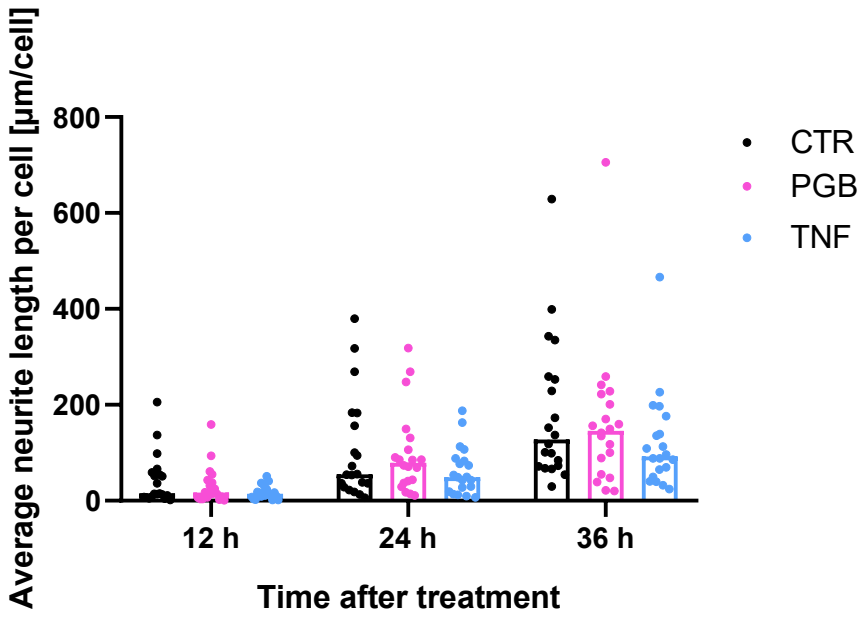

Figure 12: Average neurite outgrowth per cell on well plates – individual datapoints
Scatter graphs with bars showing the average neurite length per total number of cells. Within each timepoint the scatterplots are from left to right: control (black), treated with PGB (pink) and treated with TNF (blue). The bar marks the medium.

In figure 12 the neurite length of each image was divided by the total count of cells per image to obtain the average neurite length per cell. These individual datapoints are displayed for each condition and timepoint. The sample distributions are positively skewed and contain large outliers. At 24h and 36h after treatment the medians of the cells treated with PGB are slightly higher than the medians of the other groups. TNF is at all timepoints at the lowest average neurite length per cell compared to the other groups.

3.1.2 Neurite length independent experiments

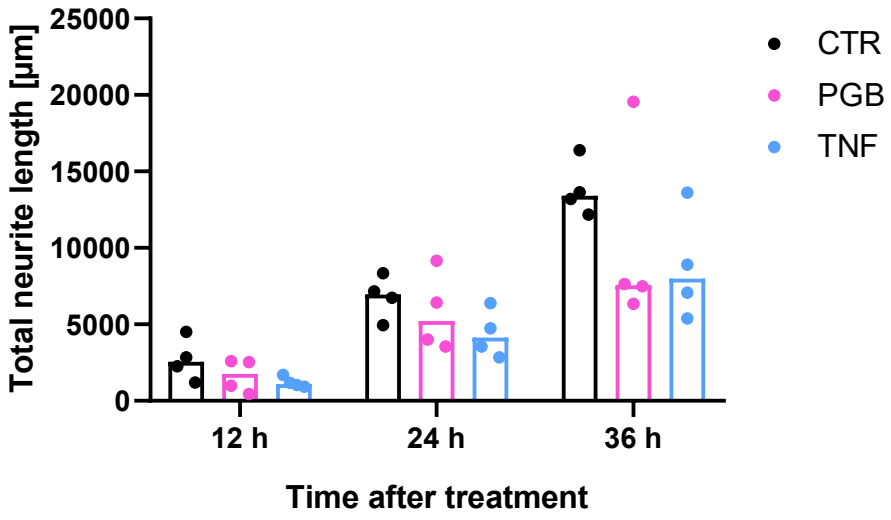

Figure 13: Total neurite length
The control group is pictured in black, PGB in pink and TNF in blue. Each point represents the sum of neurite lengths of five images of one independent experiment. The bars show the medians. The x-axis shows the different timepoints neurites were measured after treatment of the neurons in the well plates.

Figure 13 shows the total neurite lengths of five images per condition and timepoint of four independent experiments and their corresponding medians. Each point represents one biological replicate. The distribution of the graphs once again appears positively skewed with large outliers. Neurons measured as control show the highest values through all timepoints, while cells treated with PGB or TNF have less neurite outgrowth, this difference is more intense the longer the experiment is lasting. Between TNF and Pregabalin there is no big difference throughout all timepoints.

3.1.3 Proportion of cells growing out neurites

As already mentioned, the total count of cells per image was also collected. Additionally, every cell, which appeared to grow out neurites was counted, to obtain a possible difference in proportion through the different conditions and whether certain groups have more or less cells with neurite outgrowth.

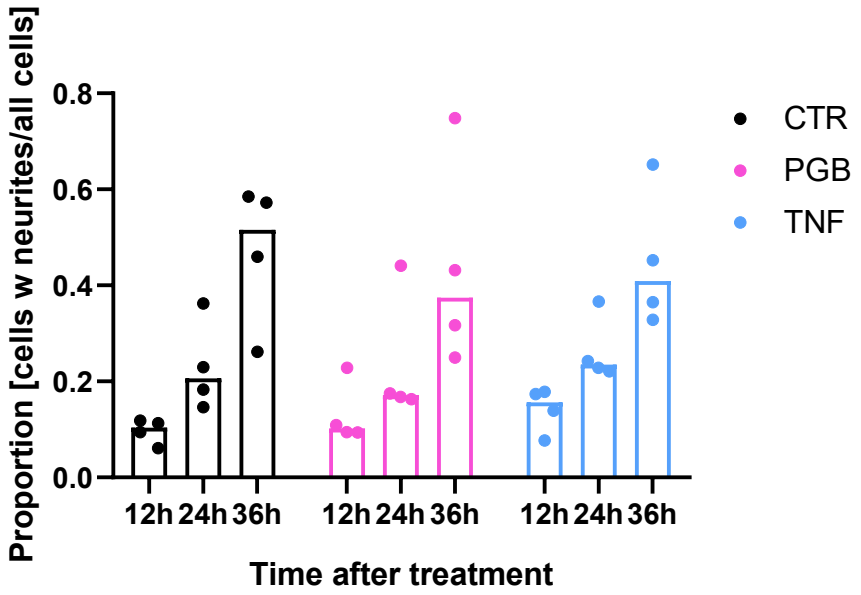

Figure 14: Proportion of cells growing out neurites
From left to right, the graph shows the proportion of cells growing out neurites of CTR group (black), PGB group (pink) and TNF group (blue) each at 12h, 24h and 36h after treatment. The bars mark the median in each group.

Figure 14 shows a proportion of cells growing out neurites in the different conditions during the different timepoints. The proportion increases for each timepoint in every condition. The values are positively skewed with many large outliers leading to the distribution appearing similar between the groups.

Calculating the neurite length data gathered from the four well plate experiments against the total count of cells showed the following results:

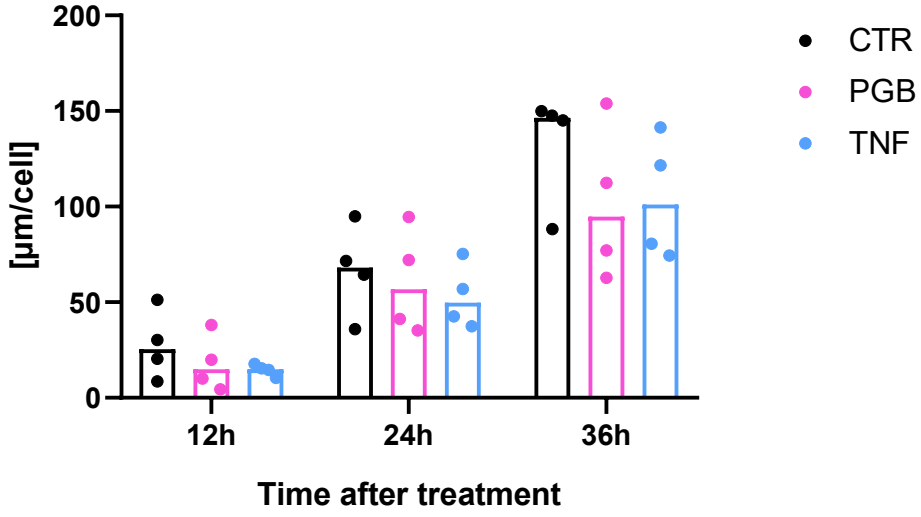

Figure 15: Average neurite length per total count of cells
This figure uses similar data as figure 12, however adds up five different images per independent experiment and therefore each experiment is presented by one point in each timepoint and condition. The bars show the median of each group.

Here in figure 15, the median of CTR is at all timepoints the highest bar, but the difference to the treatment groups appears more clearly at 24h and 36h after treatment. Pregabalin and TNF are not really distinguishable. Considering the many outliers, the distribution once again is positively skewed.

Additionally, the well plate experiments neurite length data was also compared to the total count of cells growing neurites.

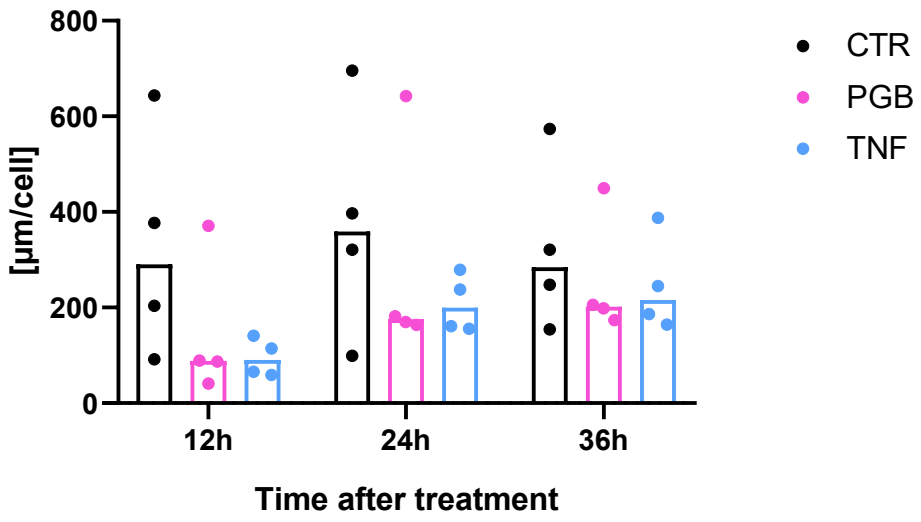

Figure 16: Average neurite length per count of cells with neurites
The graph shows the values of the average neurite length per total count of cells growing neurites of five different images per experiment. Each biological replate is represented by one point; the bars picture the medians of each group.

Figure 16 shows the medians resulting out of the average neurite length per image divided through the count of neurons which grew out neurites at the respective timepoint. Again, the control group median has the highest value at all measured timepoints. Especially at earlier timepoints, the control group shows fairly great differences to both the treatment groups. Both PGB and TNF stay at similar more low-level values. In all groups there are many outliers present.

3.2 Neurite Outgrowth in Microfluidic Devices

The outgrowth experiments in the XonaChips were repeated four times. For each experiment the DRG neurons of two mice were divided to three devices and the treatment was applied 48h after seeding the neurons into the devices.

The total neurite lengths per device of 12h and 36h after treatment were measured. One graph shows the total difference between the two timepoints here described as “absolute growth”. Additionally, the “relative growth” was assessed, meaning the percentage growth from 12h to 36h after treatment.

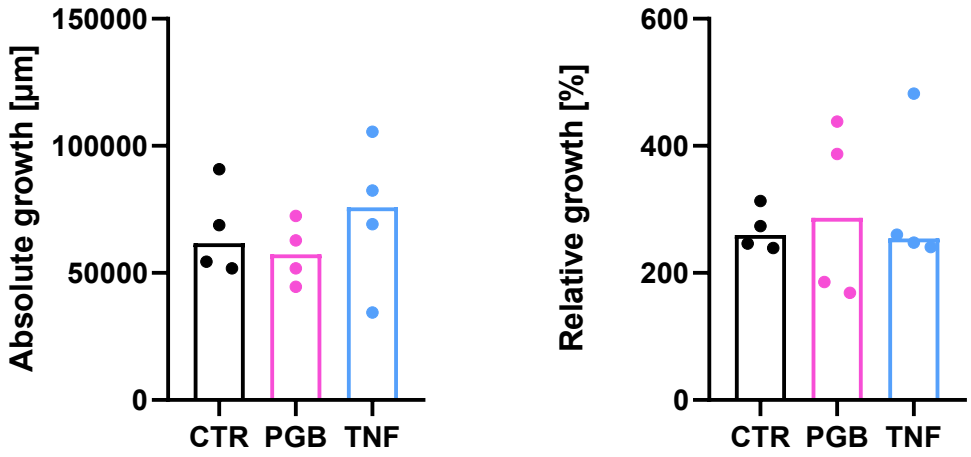

Figure 17: Neurite outgrowth in microfluidic devices
The left shows the absolute growth, meaning the difference of the neurite lengths of each device between 12h and 36h after treatment. Four values each stand for four biological replicates.
On the right, the relative growth in percent from 12h to 36h after treatment is displayed.
Detailed description in the text.

Overall, both graphs show a positively skewed distribution with large outliers, which makes the medians of the data show up at similar values.

Considering the absolute growth between the two mentioned timepoints of each device and experiment, the bars of the different conditions appear more or less at the same level. Only the median of the absolute growth of the TNF treatment appears slightly higher than the other treatment groups.

The relative growth chart also shows no great difference between the different conditions. The medians of the different treatments even are closer together compared to the absolute growth graph, where total growth differences between the timepoints are shown.

4 Discussion

It became apparent during the analysis of the acquired data of these experiments, that the way of displaying the data in graphs can show off quite opposite effects. Hence, it was of particular interest to present the data here in both ways. First, the difference between individual datapoints and averages per biological experiment is discussed and then the potential effects of the different treatments are explored.

4.1 Analysis per individual datapoints versus biological replicates

Presenting the same data in two different ways showed different results. One way, as demonstrated in figure 12, was by looking at individual datapoints resulting from the division of the neurite lengths of each analyzed image through the total count of cells of the respective image. This way of presenting the data lead to 20 datapoints for each condition without taking the four different replicate experiments in account. Displayed like this, the graph disregards the variability of different individual cell culture experiments. However, displaying individual datapoints here really shows how the individual measurements consist of many large outliers, which does not come out that clearly by showing values per independent experiment.

On the other hand, like in figure 15, the data was presented strictly based on each biological replicate. By calculating the data in that way, only four values per condition and timepoint were collected. That showed that the values of the different experiments were positively skewed suggesting that the variability between the single experiments was quite high. Therefore, predications need to be made very cautious and ideally more repetitions of experiments should be executed to be able to predict a more secure interpretation of this data.

The importance of the correct way of calculating the data is shown by the example of the results of PGB:

Considering the individual datapoints (Figure 12), PGB appears to have a slight outgrowth-stimulating effect on the neurons compared to the other groups. On the contrary (Figure 15), a clear outgrowth-inhibiting effect is shown when biological replicates are displayed. These contrary results could be possibly due to the Simpson's paradox, a statistical phenomenon appearing when data is either compared at group or individual level resulting in opposite effects. A Simpson's paradox can arise

through not considering certain confounding factors (Mangalam & Kelty-Stephen, 2021).
Therefore, potential confounders should be evaluated. They could potentially include the chosen method of analysis, speed and quality of tissue isolation, overall execution of the primary cell culture, time of the culture plate outside of the incubator for imaging and the reproducibility of the same cell density in every well of the culture plate.

To not overlook the important influencing factor of independent experiments all other results, except figure 12, are presented in values per biological replicate.

4.2 Outgrowth in well plates versus devices

Due to the limited number of replicate experiments, generally, only tendencies can be suggested.

4.2.1 Effects of tumor necrosis factor on neurite outgrowth

The results of TNF in the well plate outgrowth experiments show with some exceptions a clear tendency of TNF to supposedly inhibit neurite outgrowth compared to the control (Figure 13, 15 and 16). As a consequence of presenting the data in different ways, e.g., only neurite length in figure 13 or neurite length divided through the total count of cells or all the cells growing neurites (figure 15 and 16), the power of the inhibiting effect on neurite outgrowth seems to vary through the different timepoints. According to figure 13 and 15, the decreased neurite length is most prominent the longer the experiment lasted, at 36h after treatment the difference between the two conditions is the greatest of all measured timepoints. In figure 16, where neurite length is based on the count of the cells growing neurites, the difference between the control and TNF is most noticeable at 12h and the further along the experiment, the less difference is visible.

However, the graph of the proportion of cells with neurites (Figure 14) displayed the different treatment groups (either TNF, PGB or control) to be not very distinguishable. This evokes the possible conclusion, that the difference of the potency of TNF's inhibiting effect at the different timepoints in figure 15 and 16 is not that impactful as it may seem as they both also involve the same cell counts. There appears the possi-

bility, that these differences are due to varying cell densities analyzed on the cell plates rather than due to a real effect. Hence, giving the results of figure 13 more importance than figure 15 and 16 should be considered.

Yet, considering the experiments involving microfluidic devices, where only neurites were treated with TNF (Figure 17), no outgrowth-inhibiting effect appears. On the contrary, looking at absolute growth of neurites in the chips, the TNF devices appear to have slightly longer neurites than the control devices. The relative neurite growth of the TNF group appears at the same level as the control.

In summary, experiments of this project suggest a tendency of TNF to inhibit neurite outgrowth when applied to the whole neurons, whereas when added to only neurites growing out in microfluidic devices, TNF seems to either slightly elevate neurite outgrowth or not influence it at all. Further experiments would be needed to reassure these tendencies.

In existing literature there are only studies on the effects of TNF on the entire neurons, cell soma and neurites included. There, TNF showed mostly inhibiting effects on neurite outgrowth in DRG neurons, which aligns with the tendencies of the results of the experiments on the culture well plates.

However, this comparison must be made carefully, as previously used experimental designs differ from these experiments. On one hand, most of the experiments in literature were executed with DRG from rats, either by analyzing neurite outgrowth in DRG explant culture on collagen or dissociated DRG neurons in cell culture plates (H. Kim et al., 2015; Larsson et al., 2005; Saleh et al., 2011; L. Zhang et al., 2017). Furthermore, concentrations of TNF and NGF added to the cultures present a great difference to the experiments from this project, either no NGF at all was administered, a much lower concentration of NGF or TNF was used, or a mix of different neurotrophic factors with TNF was evaluated (Gölz et al., 2006; H. Kim et al., 2015; Larsson et al., 2005; Saleh et al., 2011; L. Zhang et al., 2017). On the other hand, none of the experiments in the literature on TNF used an analysis method comparable to the one of this project. The analysis of the neurites in the mentioned studies was mostly executed through a semi-automatic analysis of fluorescence pictures,

e.g., with the ”Simple Neurite Tracer” tool in Fiji/Image J (H. Kim et al., 2015). The possibility to observe the same cells for multiple timepoints through imaging only in phase contrast, as performed in this thesis, is a unique way of quantifying neurite length.

A study of the effects of TNF, when only neurites are treated, cannot be found in literature so far. Therefore, further investigating the possible effects of TNF in microfluidic devices would be of great interest.

4.2.2 Effects of pregabalin on neurite outgrowth

To evaluate the effects of pregabalin on neurite outgrowth from the well plate experiments which were held for this project, the way of calculating and presenting data, as carried out in 4.1, is of great importance. When the data is displayed as individual datapoints (Figure 12), particularly at the 24h timepoint, PGB appears to have an outgrowth-stimulating effect compared to the control. Considering the identical data calculated as values for each biological replicate, as seen in figure 13, 15 and 16, the graphs suggest opposite effects. PGB appears to affect the neurons in an outgrowth-inhibiting way according to the total neurite length, neurite length divided through the total number of cells, or cells growing neurites. Although, the tendency varies in its distinctiveness, PGB is right next to TNF at all timepoints below the control group.

To determine a possible time-dependent inhibiting effect, meaning a potential stronger inhibition of neurite outgrowth the later the point of measurement, more experiments would be needed. However, taking in account the results of figure 13 and 15, the inhibiting effect is greatest at 36h after treatment. This could indicate a possible time-dependent effect, which would be needed to be confirmed by further investigations. Contrariwise, figure 16 portrays PGB’s effects to be most effective at 12h and 24h after treatment.

However, as already discussed in chapter 4.2.1, the possibility remains that the data of the figures 13, 15 and 16 may not be very meaningful, because it was calculated against the total count of cells and the count of cells growing neurites. This is due to the cell counts of the analyzed images in the well plate experiments, as they are heavily fluctuating from image to image. Therefore, it may be wise to focus on the

results of figure 13. That would make the possible time-dependent effect of PGB still a very interesting point to consider and to further investigate.

Effects of PGB in the microfluidic devices, meaning a possible difference of treating the cells as a whole or only the neurites, shows that considering the absolute growth or relative growth from 12h to 36h after treatment no difference to the control is evident. Hence the similarity of PGB treated devices to the control device, a different outgrowth behavior of DRG neurons between treating the cell soma and neurites with PGB compared to only the neurites can be reasoned with.

In conclusion, PGB shows at least a tendency to inhibit neurite outgrowth when applied to well plates and therefore the whole cell, whereas when only neurites are treated, the results suggest that no effect appears.

In literature, PGB has been a great object of research regarding its effects on neurons and its therapeutical effectiveness, however only a few studies investigated the possible effect of pregabalin on the neurite outgrowth of neurons so far. In fact, only one paper investigated outgrowth on regular DRG neurons. In this paper, 50 µM and 250 µM PGB influenced the neurite outgrowth of adult DRG neurons. However, the experimental design is slightly different, at 12h after treatment, the neurons were stained with fluorescent dye and were analyzed with the Imaris imaging software, which allowed the analysis of different analysis parameters. They measured the number of branches, which were significantly lower in PGB treated neurons and the length of the longest axon, which were significantly higher (Tedeschi et al., 2016).

According to this study's results, pregabalin was formerly chosen to act as a potential positive control for neurite outgrowth in DRG neurons in the experiments of this project. However, as already discussed, the results of the well plate experiment showed a contrary effect, as PGB appeared to rather inhibit neurite outgrowth. Still, taking in account the very different analysis method and parameters of the two studies (branching points/longest axon versus total neurite length), it still is possible to match these results. A possible inhibiting effect on the branching of neurites may minimize the neurite length in total, while still the longest axon can be significantly longer than in the control neurons. Therefore, it is of great interest to show this effect from anoth-

er point of view as executed in this thesis. Further research confirming this inhibiting effect and its possible physiological consequences on neurons would be important.

4.3 Limitations

The findings of this project underlie several limitations, such as having only four biological replicates for both well plate and microfluidic devices experiments and those replicates having so many varying factors. Many more limitations are present, which will be specified in this chapter.

4.3.1 Experimental design

The results of the well plate experiments and the microfluidic devices can only be compared with limitations. For both treatments, the results seem to show an inhibiting effect in the well plates, while by selectively only treating the neurites in the devices, no effect or a subtle outgrowth-stimulating effect of TNF appeared. However, the timepoint of treating the cells is very different in both settings and could have also influenced these results to be as they are now.

While neurons in the microfluidic devices were treated 48h after being seeded, neurons in the well plate received their treatment immediately after plating. This decision to immediately treat the neurons was chosen to mimic these experiments after a previously published paper which analyzed the neurite outgrowth of PGB (Tedeschi et al., 2016). Additionally, while analyzing the 36h images of the well plate experiments, it became evident, that letting the neurons grow for much longer would lead the neurites to grow into dense networks which are not traceable anymore. This would make it impossible, to treat and trace the neurites in well plates 48h after plating.

Immediately treating the neurons in microfluidic devices is not possible, because the cells first need to regrow their neurites, which takes 24-48h to grow through the 450µm microgrooves. This factor leaves these experiments with a certain inaccuracy because it remains unclear if and how strong the timepoint of treatment is affecting neurite outgrowth. To find out if freshly seeded sensory neurons react stronger to these stimuli than two days old, cultured neurons, further experiments would be needed.

4.3.2 Method of analysis

The decision to image all timepoints in phase contrast pictures to observe the growth of the same neurons overtime came with several challenges. First, there were numerous tests to automatize the recording of the images every 12h. The idea was to put the well plates and the microfluidic devices into an environmental control microscope, where humidity, temperature and CO_2 level was regulated and where the microscope would take the images every 12h automatically at previous determined positions on the well plate. This attempted timelapse posed various problems, as the Z-axis of the available microscope could not be changed throughout the different positions. It was not possible to achieve sharp images of the whole well plate without adjusting the Z-axis. Additionally, the humidity inside the environmental control device at the lowest setting was too high, which lead to condensed water on top of the area where the microfluidic chips needed to be imaged. Hence, the recording of the images was performed manually every 12h. Furthermore, the possibility of multiple staining the same neurons with Calcein-AM was also explored to receive fluorescent images at each timepoint. This test in the well plates showed a severe difference between the stained wells versus the “not-disturbed” wells. Therefore, the decision to image in phase contrast still presented itself as the best option.

Second, the analysis of the acquired images needs to be mentioned. Due to being phase contrast images, the images could not be analyzed by any of the available neurite analysis software. That resulted in the manual tracing of the neurites in the images (Chapter 2.2.7). This way of analyzing the neurites presents some disadvantages, as this analysis is very time-consuming and phase contrast images show less detail of the neurites than fluorescent images. That also makes this analysis less precise. In the vast majority of papers on neurite outgrowth, neurons were fixed and stained with a fluorescent dye and thus completely differently analyzed than in this thesis. This also leads to the results of this study being less comparable to existing literature.

However, manual tracings of neurites can be used to train a convolutional neural network (CNN), which allows after the training of the CNN, the automatic analysis of phase contrast images via a deep learning tool (Palumbo et al., 2021). This would simplify the analysis of future experiments in well plates and in microfluidic devices

but would still allow the observation of the same cells over time, which is not possible when cells are being stained with fluorescent dye.

4.3.3 Neurotrophic factors

As already mentioned, physiologically, a cocktail of different neurotrophins (NGF, NT-3, NT-4 and BDNF) interact and play an important role in proliferation, regeneration, survival of neurons (Malfait et al., 2020). That is the reason, why NGF is added by default to most sensory neuron cultures to ensure the survival and growth of the neurons after being plated in cell culture dishes. Yet, by always and only applying NGF to every culture, it remains unknown how strong the influence of NGF on neurite outgrowth is. Literature suggests that it could also be beneficial to add a cocktail of neurotrophins. It was also shown in experiments, that the neurite-outgrowth-inducing effect was stronger by adding multiple neurotrophic factors than only NGF (Jocher et al., 2018). This presents a limitation of this study in that sense, that the experiments were never executed without the addition of growth factors. The effects of both treatments researched can only be classified as effect on top of NGF's outgrowth stimulating effect. It would be of particular interest to investigate the effect of TNF and pregabalin on one hand without any neurotrophins and on the other hand with a cocktail of neurotrophins in various concentrations.

4.4 Conclusion

The aim of the project was to investigate the influence of tumor necrosis factor and pregabalin on the outgrowth of cultured DRG neurons. In contrary to most outgrowth studies in literature so far, the outgrowth of the sensory neurons for this project was tested in two ways – in conventional well plates and in microfluidic devices. Physiologically, it is particularly interesting to differentiate between treating the whole cell with neurites with stimuli as it would happen in possible painful conditions like painful IVD involving the DRG and stimulating only peripheral nerve endings which are painfully altered in conditions like SFN (Hoeijmakers et al., 2012; Lee et al., 2009). Also, many other painful conditions, like pain after nerve injury involve neurites either being damaged or degenerated. In contrast some diseases like endometriosis also induce sprouting and hyperinnervation (Arnold et al., 2012; Gangadharan et al., 2022). Additionally, inflammation and inflammatory cytokines like TNF are frequently involved in these conditions and are known to play a role in the development of chronic pain.

That makes possible effects of TNF on the outgrowth of DRG neurons especially interesting, as it could partially decipher potential mechanisms (E. Kim et al., 2019; Lee et al., 2009; Wagner & Myers, 1996).

Pregabalin's mechanism of action in the treatment of neuropathic pain has been widely investigated before, however not much research has been done on neurite outgrowth (Bauer et al., 2009; Tedeschi et al., 2016). To be able to only treat neurites isolated from their soma, microfluidic devices were used.

The findings of the experiments performed in the well plates, where neurons as a whole were treated, suggest a potential outgrowth-inhibiting effect of both TNF and PGB compared to the control neurons. This effect of both stimuli is only a tendency as the values of the biological replicates appeared positively skewed. Because only four replicates were performed for both well plates and microfluidic devices experiments, there would be a need of more repetitions of the experiments to undermine the appearing tendencies of this thesis. These results, especially regarding TNF, are supported by existing literature. The outgrowth-inhibiting effect of PGB only conditionally matches with literature, as the findings at first glance seem contrary. The method of analysis and analyzed parameters differ immensely between literature and this thesis. Nevertheless, revealing more detail about the influence of PGB on the outgrowth of neurons would lead to a greater understanding of the frequently used drug for neuropathic pain. The proportion of neurons growing neurites reveals no real difference between the two stimuli and the control group.

Considering the outcome of the experiments in the microfluidic chips, results showed that neither TNF nor PGB devices were really distinguishable in neurite length from control devices. Yet, the absolute growth of TNF compared to the control could possibly imply a slight outgrowth-stimulating effect. As the effect appears very small, this could indicate that both these stimuli more strongly affect neurons at DRG level, than only the neurites in the periphery. However, many limitations need to be considered here, as an in vitro DRG culture can never portray the complex interaction of DRG neurons in vivo, the timeframe of treatment was very different in well plates and devices experiments and only four biological replicates with many large outliers point to these findings. In addition, all experiments exclusively were carried out in the presence of only NGF, which does not portray a realistic simulation of the in vivo situation of sensory neurons. Lastly, the possibility of this manual analysis method of phase

contrast images to show different results than the general common analysis of fluorescent-dyed images is also present.

4.5 Outlook and future perspectives

Following these first experiments investigating neurite outgrowth, many future experiments could lead to more clarity. First, more replicate experiments could be performed to see if the findings of this project are true to more repetitions and the presented data gains more significance.

Second, if still interesting results are present, a modulation of the well plate experiments would also make sense to investigate the importance of the timepoint of treatment. That would mean, that the neurons would only be treated with the stimuli after a certain time after seeding, e.g., 12h, and then imaged every 12h until 36h after treatment. This way the neurons could possibly be less affected by the stimuli which would imply that immediately treated neurons react stronger than neurons, which already adhered to the culture plate for 12h. That could also mean, that the experiments in the devices show no result because of the timing of the treatment rather than the neurites reacting differently.

Third, elongating the time period in which the neurons are imaged after treatment could also be of interest, as some results showed an increasing difference to the control the longer the experiment lasted.

Fourth, by changing the method of analysis to fluorescent imaging more information could be gained, because these images show more detail than phase contrast images. Then parameters, such as branching points, length of the longest axons and others could also be collected by the neurite analysis tools available. Additionally, still analyzing consecutive phase contrast images via a deep learning tool could also bear a very interesting possibility in analyzing outgrowth without needing to analyze with the time-intense manual method described in this thesis.

Interesting future experiments with the microfluidic devices could involve keratinocytes co-cultures, where keratinocytes would be seeded into the axonal compartment and DRG neurites could grow into the keratinocytes, which would closer mimic how nerve fibers innervate the skin. Then after the treatment of the neurites with stimuli, next to the analysis of the neurites themselves, also Ca2+-imaging could be performed on the neurons to deepen the knowledge of possible molecular mechanisms behind the neurite outgrowth-inhibiting or -stimulating effects.

5 References

Arnold, J., Barcena de Arellano, M. L., Rüster, C., Vercellino, G. F., Chiantera, V., Schneider, A., & Mechsner, S. (2012). Imbalance between sympathetic and sensory innervation in peritoneal endometriosis. *Brain, Behavior, and Immunity*, *26*(1), 132–141. https://doi.org/10.1016/j.bbi.2011.08.004

Atmaramani, R., Veeramachaneni, S., Mogas, L. V., Koppikar, P., Black, B. J., Hammack, A., Pancrazio, J. J., & Granja-Vazquez, R. (2021). Investigating the Function of Adult DRG Neuron Axons Using an In Vitro Microfluidic Culture System. *Micromachines*, *12*(11), Article 11. https://doi.org/10.3390/mi12111317

Basbaum, A. I., Bautista, D. M., Scherrer, G., & Julius, D. (2009). Cellular and Molecular Mechanisms of Pain. *Cell*, *139*(2), 267–284. https://doi.org/10.1016/j.cell.2009.09.028

Bauer, C. S., Nieto-Rostro, M., Rahman, W., Tran-Van-Minh, A., Ferron, L., Douglas, L., Kadurin, I., Ranjan, Y. S., Fernandez-Alacid, L., Millar, N. S., Dickenson, A. H., Lujan, R., & Dolphin, A. C. (2009). The Increased Trafficking of the Calcium Channel Subunit α2δ-1 to Presynaptic Terminals in Neuropathic Pain Is Inhibited by the α2δ Ligand Pregabalin. *Journal of Neuroscience*, *29*(13), 4076–4088. https://doi.org/10.1523/JNEUROSCI.0356-09.2009

Belamadni, A., Ren, D., Jayaraj, N., George, D., Miller, R., & Mencihella, D. (2022). Integrating Sensory Neurons with Keratinocytes to Model Painful Diabetic Neuropathy on a Chip. *The Journal of Pain*, *23*(5), 10. https://doi.org/10.1016/j.jpain.2022.03.038

Berger, A. A., Liu, Y., Possoit, H., Rogers, A. C., Moore, W., Gress, K., Cornett, E. M., Kaye, A. D., Imani, F., Sadegi, K., Varrassi, G., Viswanath, O., & Urits, I.

(2021). Dorsal Root Ganglion (DRG) and Chronic Pain. *Anesthesiology and Pain Medicine*, *11*(2), e113020. https://doi.org/10.5812/aapm.113020

Bourinet, E., Altier, C., Hildebrand, M. E., Trang, T., Salter, M. W., & Zamponi, G. W. (2014). Calcium-permeable ion channels in pain signaling. *Physiological Reviews*, *94*(1), 81–140. https://doi.org/10.1152/physrev.00023.2013

Calandre, E. P., Rico-Villademoros, F., & Slim, M. (2016). Alpha2delta ligands, gabapentin, pregabalin and mirogabalin: A review of their clinical pharmacology and therapeutic use. *Expert Review of Neurotherapeutics*, *16*(11), 1263–1277. https://doi.org/10.1080/14737175.2016.1202764

Campenot, R. B. (1977). Local control of neurite development by nerve growth factor. *Proceedings of the National Academy of Sciences of the United States of America*, *74*(10), 4516–4519. https://doi.org/10.1073/pnas.74.10.4516

Campenot, R. B. (1979). [25] Independent control of the local environment of somas and neurites. In *Methods in Enzymology* (Vol. 58, pp. 302–307). Elsevier. https://doi.org/10.1016/S0076-6879(79)58146-4

Campenot, R. B. (1982). Development of sympathetic neurons in compartmentalized cultures: II. Local control of neurite survival by nerve growth factor. *Developmental Biology*, *93*(1), 13–21. https://doi.org/10.1016/0012-1606(82)90233-0

Campenot, R. B. (1994). NGF and the local control of nerve terminal growth. *Journal of Neurobiology*, *25*(6), 599–611. https://doi.org/10.1002/neu.480250603

Chao, M. V. (2003). Neurotrophins and their receptors: A convergence point for many signalling pathways. *Nature Reviews Neuroscience*, *4*(4), Article 4. https://doi.org/10.1038/nrn1078

Clark, A. J., Menendez, G., AlQatari, M., Patel, N., Arstad, E., Schiavo, G., & Koltzenburg, M. (2018). Functional imaging in microfluidic chambers reveals

sensory neuron sensitivity is differentially regulated between neuronal regions. *PAIN*, *159*(7), 1413–1425. https://doi.org/10.1097/j.pain.0000000000001145

Cohen, S. P., Vase, L., & Hooten, W. M. (2021). Chronic pain: An update on burden, best practices, and new advances. *The Lancet*, *397*(10289), 2082–2097. https://doi.org/10.1016/S0140-6736(21)00393-7

de Macedo, F. H. P., Aires, R. D., Fonseca, E. G., Ferreira, R. C. M., Machado, D. P. D., Chen, L., Zhang, F.-X., Souza, I. A., Lemos, V. S., Romero, T. R. L., Moutal, A., Khanna, R., Zamponi, G. W., & Cruz, J. S. (2019). TNF-α mediated up-regulation of NaV1.7 currents in rat dorsal root ganglion neurons is independent of CRMP2 SUMOylation. *Molecular Brain*, *12*(1), 117. https://doi.org/10.1186/s13041-019-0538-0

Freemont, A. J., Peacock, T. E., Goupille, P., Hoyland, J. A., O'Brien, J., & Jayson, M. I. V. (1997). Nerve ingrowth into diseased intervertebral disc in chronic back pain. *The Lancet*, *350*(9072), 178–181. https://doi.org/10.1016/S0140-6736(97)02135-1

Gangadharan, V., Zheng, H., Taberner, F. J., Landry, J., Nees, T. A., Pistolic, J., Agarwal, N., Männich, D., Benes, V., Helmstaedter, M., Ommer, B., Lechner, S. G., Kuner, T., & Kuner, R. (2022). Neuropathic pain caused by miswiring and abnormal end organ targeting. *Nature*, *606*(7912), Article 7912. https://doi.org/10.1038/s41586-022-04777-z

Gölz, G., Uhlmann, L., Lüdecke, D., Markgraf, N., Nitsch, R., & Hendrix, S. (2006). The cytokine/neurotrophin axis in peripheral axon outgrowth. *The European Journal of Neuroscience*, *24*(10), 2721–2730. https://doi.org/10.1111/j.1460-9568.2006.05155.x

Griffin, J. W., Pan, B., Polley, M. A., Hoffman, P. N., & Farah, M. H. (2010). Measuring nerve regeneration in the mouse. *Experimental Neurology*, *223*(1), 60–71. https://doi.org/10.1016/j.expneurol.2009.12.033

Hoeijmakers, J. G., Faber, C. G., Lauria, G., Merkies, I. S., & Waxman, S. G. (2012). Small-fibre neuropathies—Advances in diagnosis, pathophysiology and management. *Nature Reviews Neurology*, *8*(7), Article 7. https://doi.org/10.1038/nrneurol.2012.97

Holt, E., Stanton-Turcotte, D., & Iulianella, A. (2021). Development of the Vertebrate Trunk Sensory System: Origins, Specification, Axon Guidance, and Central Connectivity. *Neuroscience*, *458*, 229–243. https://doi.org/10.1016/j.neuroscience.2020.12.037

Ji, R.-R., Chamessian, A., & Zhang, Y.-Q. (2016). Pain regulation by non-neuronal cells and inflammation. *Science (New York, N.Y.)*, *354*(6312), 572–577. https://doi.org/10.1126/science.aaf8924

Ji, R.-R., Xu, Z.-Z., & Gao, Y.-J. (2014). Emerging targets in neuroinflammation-driven chronic pain. *Nature Reviews. Drug Discovery*, *13*(7), 533–548. https://doi.org/10.1038/nrd4334

Jocher, G., Mannschatz, S. H., Offterdinger, M., & Schweigreiter, R. (2018). Microfluidics of Small-Population Neurons Allows for a Precise Quantification of the Peripheral Axonal Growth State. *Frontiers in Cellular Neuroscience*, *12*. https://www.frontiersin.org/articles/10.3389/fncel.2018.00166

Junger, H., & Sorkin, L. S. (2000). Nociceptive and inflammatory effects of subcutaneous TNFα. *PAIN*, *85*(1), 145–151. https://doi.org/10.1016/S0304-3959(99)00262-6

Karten, B., Hayashi, H., Campenot, R. B., Vance, D. E., & Vance, J. E. (2005). Neuronal models for studying lipid metabolism and transport. *Methods*, *36*(2), 117–128. https://doi.org/10.1016/j.ymeth.2004.11.004

Kato, K., Liu, H., Kikuchi, S., Myers, R. R., & Shubayev, V. I. (2010). Immediate anti-tumor necrosis factor-alpha (etanercept) therapy enhances axonal regeneration after sciatic nerve crush. *Journal of Neuroscience Research*, *88*(2), 360–368. https://doi.org/10.1002/jnr.22202

Kim, E., Hwang, S.-H., Kim, H.-K., Abdi, S., & Kim, H. K. (2019). Losartan, an Angiotensin II Type 1 Receptor Antagonist, Alleviates Mechanical Hyperalgesia in a Rat Model of Chemotherapy-Induced Neuropathic Pain by Inhibiting Inflammatory Cytokines in the Dorsal Root Ganglia. *Molecular Neurobiology*, *56*(11), 7408–7419. https://doi.org/10.1007/s12035-019-1616-0

Kim, H., Caspar, T. W., Shah, S. B., & Hsieh, A. H. (2015). Effects of proinflammatory cytokines on axonal outgrowth from adult rat lumbar dorsal root ganglia using a novel three-dimensional culture system. *The Spine Journal*, *15*(8), 1823–1831. https://doi.org/10.1016/j.spinee.2015.03.017

Koncina, E., Roth, L., Gonthier, B., & Bagnard, D. (2007). Role of Semaphorins during Axon Growth and Guidance. In D. Bagnard (Ed.), *Axon Growth and Guidance* (pp. 50–64). Springer. https://doi.org/10.1007/978-0-387-76715-4_4

Kramer, T., Greco, T. M., Taylor, M. P., Ambrosini, A. E., Cristea, I. M., & Enquist, L. W. (2012). Kinesin-3 Mediates Axonal Sorting and Directional Transport of Alphaherpesvirus Particles in Neurons. *Cell Host & Microbe*, *12*(6), 806–814. https://doi.org/10.1016/j.chom.2012.10.013

Kreß, L., Hofmann, L., Klein, T., Klug, K., Saffer, N., Spitzel, M., Bär, F., Sommer, C., Karl, F., & Üçeyler, N. (2021). Differential impact of keratinocytes and fibro-

blasts on nociceptor degeneration and sensitization in small fiber neuropathy. *PAIN*, *162*(4), 1262–1272. https://doi.org/10.1097/j.pain.0000000000002122

Larsson, K., Rydevik, B., & Olmarker, K. (2005). Disc related cytokines inhibit axonal outgrowth from dorsal root ganglion cells in vitro. *Spine*, *30*(6), 621–624. https://doi.org/10.1097/01.brs.0000155410.48700.9e

Lee, S., Moon, C. S., Sul, D., Lee, J., Bae, M., Hong, Y., Lee, M., Choi, S., Derby, R., Kim, B.-J., Kim, J., Yoon, J.-S., Wolfer, L., Kim, J., Wang, J., Hwang, S.-W., & Lee, S.-H. (2009). Comparison of growth factor and cytokine expression in patients with degenerated disc disease and herniated nucleus pulposus. *Clinical Biochemistry*, *42*(15), 1504–1511. https://doi.org/10.1016/j.clinbiochem.2009.06.017

Li, Z., Taylor, C. P., Weber, M., Piechan, J., Prior, F., Bian, F., Cui, M., Hoffman, D., & Donevan, S. (2011). Pregabalin is a potent and selective ligand for α2δ-1 and α2δ-2 calcium channel subunits. *European Journal of Pharmacology*, *667*(1), 80–90. https://doi.org/10.1016/j.ejphar.2011.05.054

Luo, Z. D., Chaplan, S. R., Higuera, E. S., Sorkin, L. S., Stauderman, K. A., Williams, M. E., & Yaksh, T. L. (2001). Upregulation of Dorsal Root Ganglion α2δ Calcium Channel Subunit and Its Correlation with Allodynia in Spinal Nerve-Injured Rats. *Journal of Neuroscience*, *21*(6), 1868–1875. https://doi.org/10.1523/JNEUROSCI.21-06-01868.2001

Malfait, A.-M., Miller, R. E., & Block, J. A. (2020). Targeting neurotrophic factors: Novel approaches to musculoskeletal pain. *Pharmacology & Therapeutics*, *211*, 107553. https://doi.org/10.1016/j.pharmthera.2020.107553

Malik, K. M., Imani, F., Beckerly, R., & Chovatiya, R. (2020). Risk of Opioid Use Disorder from Exposure to Opioids in the Perioperative Period: A Systematic Re-

view. *Anesthesiology and Pain Medicine*, *10*(1), Article 1. https://doi.org/10.5812/aapm.101339

Mangalam, M., & Kelty-Stephen, D. G. (2021). Point estimates, Simpson's paradox, and nonergodicity in biological sciences. *Neuroscience and Biobehavioral Reviews*, *125*, 98–107. https://doi.org/10.1016/j.neubiorev.2021.02.017

Mantyh, W. G., Jimenez-Andrade, J. M., Stake, J. I., Bloom, A. P., Kaczmarska, M. J., Taylor, R. N., Freeman, K. T., Ghilardi, J. R., Kuskowski, M. A., & Mantyh, P. W. (2010). Blockade of nerve sprouting and neuroma formation markedly attenuates the development of late stage cancer pain. *Neuroscience*, *171*(2), 588–598. https://doi.org/10.1016/j.neuroscience.2010.08.056

Martínez, A. L., Brea, J., Barro, M., Monroy, X., Merlos, M., Burgueño, J., & Loza, M. I. (2021). Development of a novel in vitro assay to screen for neuroprotective drugs against iatrogenic neurite shortening. *PloS One*, *16*(3), e0248139. https://doi.org/10.1371/journal.pone.0248139

Matsuda, M., Huh, Y., & Ji, R.-R. (2019). Roles of inflammation, neurogenic inflammation, and neuroinflammation in pain. *Journal of Anesthesia*, *33*(1), 131–139. https://doi.org/10.1007/s00540-018-2579-4

Millet, L. J., & Gillette, M. U. (2012). Over a century of neuron culture: From the hanging drop to microfluidic devices. *The Yale Journal of Biology and Medicine*, *85*(4), 501–521.

Mohd Isa, I. L., Teoh, S. L., Mohd Nor, N. H., & Mokhtar, S. A. (2023). Discogenic Low Back Pain: Anatomy, Pathophysiology and Treatments of Intervertebral Disc Degeneration. *International Journal of Molecular Sciences*, *24*(1), Article 1. https://doi.org/10.3390/ijms24010208

Mukhopadhyay, R. (2007). When PDMS isn't the best. *Analytical Chemistry*, *79*(9), 3248–3253. https://doi.org/10.1021/ac071903e

Nagendran, T., Poole, V., Harris, J., & Taylor, A. M. (2018). Use of Pre-Assembled Plastic Microfluidic Chips for Compartmentalizing Primary Murine Neurons. *Journal of Visualized Experiments: JoVE*, *141*. https://doi.org/10.3791/58421

Ogon, I., Takebayashi, T., Takashima, H., Tanimoto, K., Ida, K., Yoshimoto, M., Fujiwara, H., Kubo, T., & Yamashita, T. (2015). Analysis of chronic low back pain with magnetic resonance imaging T2 mapping of lumbar intervertebral disc. *Journal of Orthopaedic Science*, *20*(2), 295–301. https://doi.org/10.1007/s00776-014-0686-0

Palumbo, A., Grüning, P., Landt, S. K., Heckmann, L. E., Bartram, L., Pabst, A., Flory, C., Ikhsan, M., Pietsch, S., Schulz, R., Kren, C., Koop, N., Boltze, J., Madany Mamlouk, A., & Zille, M. (2021). Deep Learning to Decipher the Progression and Morphology of Axonal Degeneration. *Cells*, *10*(10), Article 10. https://doi.org/10.3390/cells10102539

Paranjape, S. R., Nagendran, T., Poole, V., Harris, J., & Taylor, A. M. (2019). Compartmentalization of Human Stem Cell-Derived Neurons within Pre-Assembled Plastic Microfluidic Chips. *Journal of Visualized Experiments: JoVE*, *147*. https://doi.org/10.3791/59250

Park, S. H., Eber, M. R., Fonseca, M. M., Patel, C. M., Cunnane, K. A., Ding, H., Hsu, F.-C., Peters, C. M., Ko, M.-C., Strowd, R. E., Wilson, J. A., Hsu, W., Romero-Sandoval, E. A., & Shiozawa, Y. (2021). Usefulness of the measurement of neurite outgrowth of primary sensory neurons to study cancer-related painful complications. *Biochemical Pharmacology*, *188*, 114520. https://doi.org/10.1016/j.bcp.2021.114520

Raja, S. N., Carr, D. B., Cohen, M., Finnerup, N. B., Flor, H., Gibson, S., Keefe, F. J., Mogil, J. S., Ringkamp, M., Sluka, K. A., Song, X.-J., Stevens, B., Sullivan, M. D., Tutelman, P. R., Ushida, T., & Vader, K. (2020). The revised International

Association for the Study of Pain definition of pain: Concepts, challenges, and compromises. *Pain*, *161*(9), 1976–1982. https://doi.org/10.1097/j.pain.0000000000001939

Saleh, A., Smith, D. R., Balakrishnan, S., Dunn, L., Martens, C., Tweed, C. W., & Fernyhough, P. (2011). Tumor necrosis factor-α elevates neurite outgrowth through an NF-κB-dependent pathway in cultured adult sensory neurons: Diminished expression in diabetes may contribute to sensory neuropathy. *Brain Research*, *1423*, 87–95. https://doi.org/10.1016/j.brainres.2011.09.029

Segelcke, D., Fischer, H. K., Hütte, M., Dennerlein, S., Benseler, F., Brose, N., Pogatzki-Zahn, E. M., & Schmidt, M. (2021). Tmem160 contributes to the establishment of discrete nerve injury-induced pain behaviors in male mice. *Cell Reports*, *37*(12), 110152. https://doi.org/10.1016/j.celrep.2021.110152

Shu, X.-Q., & Mendell, L. M. (1999). Neurotrophins and hyperalgesia. *Proceedings of the National Academy of Sciences*, *96*(14), 7693–7696. https://doi.org/10.1073/pnas.96.14.7693

Sommer, C., Leinders, M., & Üçeyler, N. (2018). Inflammation in the pathophysiology of neuropathic pain. *PAIN*, *159*(3), 595–602. https://doi.org/10.1097/j.pain.0000000000001122

Tedeschi, A., Dupraz, S., Laskowski, C. J., Xue, J., Ulas, T., Beyer, M., Schultze, J. L., & Bradke, F. (2016). The Calcium Channel Subunit Alpha2delta2 Suppresses Axon Regeneration in the Adult CNS. *Neuron*, *92*(2), 419–434. https://doi.org/10.1016/j.neuron.2016.09.026

Tsantoulas, C., Farmer, C., Machado, P., Baba, K., McMahon, S. B., & Raouf, R. (2013). Probing functional properties of nociceptive axons using a microfluidic culture system. *PloS One*, *8*(11), e80722. https://doi.org/10.1371/journal.pone.0080722

Vysokov, N., McMahon, S. B., & Raouf, R. (2019). The role of NaV channels in synaptic transmission after axotomy in a microfluidic culture platform. *Scientific Reports*, *9*(1), Article 1. https://doi.org/10.1038/s41598-019-49214-w

Wagner, R., & Myers, R. R. (1996). Endoneurial injection of TNF-alpha produces neuropathic pain behaviors. *Neuroreport*, *7*(18), 2897–2901. https://doi.org/10.1097/00001756-199611250-00018

Wang, Y., Wang, S., Wu, H., Liu, X., Ma, J., Khan, M. A., Riaz, A., Wang, L., Qiu, H.-J., & Sun, Y. (2020). Compartmentalized Neuronal Culture for Viral Transport Research. *Frontiers in Microbiology*, *11*, 1470. https://doi.org/10.3389/fmicb.2020.01470

Wei, J., Su, W., Zhao, Y., Wei, Z., Hua, Y., Xue, P., Zhu, X., Chen, Y., & Chen, G. (2022). Maresin 1 promotes nerve regeneration and alleviates neuropathic pain after nerve injury. *Journal of Neuroinflammation*, *19*(1), 32. https://doi.org/10.1186/s12974-022-02405-1

Wei, S., Qiu, C.-Y., Jin, Y., Liu, T.-T., & Hu, W.-P. (2021). TNF-α acutely enhances acid-sensing ion channel currents in rat dorsal root ganglion neurons via a p38 MAPK pathway. *Journal of Neuroinflammation*, *18*(1), 92. https://doi.org/10.1186/s12974-021-02151-w

Xiao, W. H., & Bennett, G. J. (2008). Chemotherapy-evoked neuropathic pain: Abnormal spontaneous discharge in A-fiber and C-fiber primary afferent neurons and its suppression by acetyl-l-carnitine. *PAIN*, *135*(3), 262–270. https://doi.org/10.1016/j.pain.2007.06.001

Xona Microfluidics, Inc. (2020). *XonaChips 2-Compartment XC Series Protocol*. https://xonamicrofluidics.com/protocols/

Yan, D., Liu, X., & Guo, S.-W. (2017). Endometriosis-Derived Thromboxane A2 Induces Neurite Outgrowth. *Reproductive Sciences (Thousand Oaks, Calif.)*, *24*(6), 829–835. https://doi.org/10.1177/1933719116670037

Zhang, J.-M., & An, J. (2007). Cytokines, inflammation, and pain. *International Anesthesiology Clinics*, *45*(2), 27–37. https://doi.org/10.1097/AIA.0b013e318034194e

Zhang, L., Yue, Y., Ouyang, M., Liu, H., & Li, Z. (2017). The Effects of IGF-1 on TNF-α-Treated DRG Neurons by Modulating ATF3 and GAP-43 Expression via PI3K/Akt/S6K Signaling Pathway. *Neurochemical Research*, *42*(5), 1403–1421. https://doi.org/10.1007/s11064-017-2192-1

Acknowledgement

First of all, I would like to thank Prof. Dr. Manuela Schmidt for offering me to write my master thesis in her research group. I really appreciated the possibility to deep dive into such an interesting masters project in neuroscience and I was thankful for the opportunity to be able to plan and perform these interesting experiments with her continuous guidance and support.

Furthermore, I would like to thank Ass.-Prof. Dr. Marietta Zille for constantly supporting me with her great expertise starting from the planning of experiments, developing solutions for imaging issues to working out the proper analysis method for my data. I really was able to benefit from her impressive problem-solving skills making it possible for my master thesis project to work out like it did.

Many thanks to Hanna Fischer, Daniela Schmidt Garcia and Sabrina Grundtner for showing me very patiently how to do the practical part of my thesis. Moreover, I am very thankful for getting to know all of you.
Thanks to Lea, my fellow master student in the lab, I appreciated sharing this interesting time with you.
Thanks to Dr. David Gomez-Varela, I could really benefit from discussing my experiments in such a great round table of highly skilled scientists.
Also thank you to Dr. Julia Sondermann and Dr. Feng Xian for your highly appreciated advice. Thank you to the whole Systems Biology of Pain Lab for the pleasant lab-environment and for always helping me whenever I needed something.

Furthermore, thanks to my parents for the constant encouragement and support during my studies. Many thanks to my brother-in-law and my sister for proofreading my thesis and for their continuous moral support.
Finally, very special thanks to Lena und Lina for always being there for me, proofreading and keeping me sane and entertained during my studies.

Appendix

XonaChip DRG culture protocol

- Adaption of the original XonaChip and DRG culture with WT mouse protocol

Equipment and Supplies Needed:

- o 1 four-well-plate, one well filled with 3 ml sterile water
- o 37ºC 5% CO2 incubator
- o bio-safety cabinet
- o 400µl XC Pre-Coat or 70% EtOH per chip
- o 3-4 ml PBS
- o 400µl PDL (1mg/ml) per chip
- o 400µl Laminin (20µg/ml) per chip
- o Medium + 100ng/ml NGF (per chip 500µl medium needed)
- o 70% EtOH for troubleshooting if needed
- o For DRG digestion – see WT DRG culture protocol
- o Small beaker for liquid waste (from washing and coating steps)

XonaChip: LEFT side is Cell/Somal Side and the RIGHT side as Axonal Side

Prepare in hood (for chips and cell culture)

- o One eppi with 1ml of fresh serum-free medium per mouse (DMEM/F-12+GlutaMax)
- o One 15ml falcon with 2,5ml serum-free medium per mouse (papain digest)
- o One 15ml falcon tube with 2ml medium with serum per mouse (for trituration) + 1-2 ml for preconditioning the Chips with Well
- o One 15ml falcon tube with 5ml medium to add 5ml aliquot of NGF to

Preparing and Coating the XonaChip:

Be careful not to withdraw all the liquid out of the channels of the XonaChip. Always leave liquid in the main channels! Be careful not to introduce air bubbles into the main channels or microgrooves. See troubleshooting guide if bubbles form.

1. In the hood, place the XonaChip into a petri dish.

2. Add 100µl of XC Pre-Coat to the upper left well of the XonaChip and allow it to flow through the main channel into the adjoining well. Wait 1 min.
3. Fill the lower left well with 100µl of XC Pre-Coat. Wait 5 min to allow the solution to flow through the microgrooves.
4. Add 100µl of XC Pre-Coat to the upper right well. Wait 1 min.
5. Fill the lower right well with 100µl of XC Pre-Coat. Wait 5 min.
6. Aspirate the solution from each well – always angle the pipet tip away from the main channel entrance. DO NOT INTRODUCE BUBBLES.
Immediately add 150µl of PBS to the upper left well. Wait 1 min.
7. Fill the lower left well with PBS (~100-150µl). Wait 5 min to allow liquids to flow through the microgrooves.
8. Add 150µl 1X PBS to the upper right well. Wait 1 min.
9. Fill the lower right well with PBS (~100-150µl). Wait 3 min.
10. Repeat steps 6-9 for a second PBS wash.
11. Check the device for bubbles in the channels. If bubbles appear, refer to the troubleshooting guide.
12. Aspirate the solution from each well.
13. Add 100µl of PDL to the upper left well of the XonaChip. Wait 1 min. Fill the lower left well with 100µl of PDL. Wait 5 min.
14. Add 100µl of PDL to the upper right well of the XonaChip. Wait 1 min. Add 100µl to the lower right well.
15. Close the petri dish to prevent evaporation and place the XonaChip containing PDL in an incubator at 37°C for 1,5h.

Put eppi with serum-free medium next to dissection scope.
Place Collagenase into the hood to warm up to RT.
Dissection of the mouse. Isolate all DRG neurons and put them in eppi with serum-free medium.

Continue Digestion of the DRG & BSA column like in the cell culture protocol.
After 1,5h incubation time:
16. Aspirate the PDL from the device.
17. Add 100µl of Laminin to the upper left well of the Chip. Wait 1. min. Fill the lower left well with 100µl of laminin. Wait 5 min.

18. Add 100µl of Laminin to the upper right well of the Chip. Wait 1 min. Add 100µl to the lower right well.
19. Close the petri dish to prevent evaporation and place the Chip containing Laminin in an incubator at 37°C for 30 min.
20. Repeat the 1X PBS wash steps 6-9 twice to remove excess laminin.
21. Immediately add 100µl of cell culture media to the upper left well of the Chip. Wait 1 min. Add media to the lower left well. Wait 5 min. Add media to the upper right well. Wait 1 min. Add 100µl medium to the lower right well of the XonaChip.
22. Store pre-conditioned XonaChip in a 37ºC 5% CO2 incubator until ready for loading neurons.

Note: If you are unable to load neurons into the XonaChip the same day it is best to follow steps 1-11 and incubate the PDL for 4h in a 37ºC 5% CO2 incubator, rinse twice with PBS, wrap the petri dish with parafilm, and store at 4°C up to 2 weeks.

Seeding DRG neurons into the Chip:
1. Resuspend cells in proper amount of media with NGF. 10-20 µl cell suspension is needed for one chip.
2. Aspirate the media out of the wells of the Chip by angling the tip away of the main channel entrance. Ensure media remains in the main channels at all times. Never remove media from the main channels.
3. Load 10µl of primary neurons on the left side of the XonaChip. Add primary neurons directly into the channels by angling the pipette towards the entrance of the channel and slowly dispensing the cell suspension. Alternatively, the cell suspension can be split into two aliquots of 5µl and be added into upper and lower left well.
Check under a microscope to ensure the neurons are flowing into the Chip’s main channel. Wait for 20 min to allow the cells to attach.
3. Add 150µl simultaneously to both somal wells, and then add 100µl simultaneously to both axonal wells. (Use P1000 and P200), so that the cells don’t get flushed out of the main channel from one side.
Return the XonaChip to the incubator.
4. After 24-48h, perform a media change by removing media from the wells only. Make sure the channel remains filled. Add media in different amounts according to fluidic isolation.

5. Media will need to be monitored every 1-2 days and changed as needed. Keep an eye on level of media in the Chip, if a lot of evaporation is going on, add 30 ml of media simultaneously to somal wells (left side) and simultaneously to axonal wells (right side).

Troubleshooting guide if bubbles occur during washing steps:

Aspirate PBS from wells angling the pipet tip away from the channel opening.

Dispense 100 µl of EtOH 70% into upper left well, angling the tip of the pipet near the channel opening. Wait 1 min.

Fill the lower left well with 100 µl 70% EtOH angling the pipet away from the main channels and slowly dispense the liquid. Wait 5 min to allow liquids to flow through the microgrooves.

Add 100µl of 70% EtOH to upper right well, angling the pipet tip near the channel entrance. Wait 1 min.

Fill the lower right well with 100 µl EtOH 70% angling the pipet tip away from the channel entrance. Wait 5 min.

Continue with step 6.

Data tables

Individual datapoints data

Average neurite length per cell - Individual datapoints [µm/cell]				
		12h	**24h**	**36h**
Experiment 1	CTR	54.15009	269.1941	628.6797
Experiment 1	CTR	8.420429	18.17283	67.67454
Experiment 1	CTR	7.159281	13.13069	71.65809
Experiment 1	CTR	205.9768	379.422	342.7498
Experiment 1	CTR	11.01883	55.73697	118.5417
Experiment 2	CTR	51.8686	182.8264	334.707
Experiment 2	CTR	36.56789	36.13121	29.59386
Experiment 2	CTR	58.96667	100.5392	152.3244
Experiment 2	CTR	50.86711	94.64189	173.0608
Experiment 2	CTR	66.39544	156.3281	258.7793
Experiment 3	CTR	1.976098	6.539686	66.58855
Experiment 3	CTR	98.36256	183.6748	229.2549
Experiment 3	CTR	14.62378	72.34422	252.8549
Experiment 3	CTR	7.530364	53.64918	136.8977
Experiment 3	CTR	136.9266	317.5407	399.0307
Experiment 4	CTR	13.72059	54.20344	100.6931
Experiment 4	CTR	4.686706	36.34041	98.89641
Experiment 4	CTR	15.09533	38.31333	54.26833
Experiment 4	CTR	12.69775	22.24875	73.19567
Experiment 4	CTR	4.195364	28.56702	84.58069
Experiment 1	PGB	60.984	247.521	200.8153
Experiment 1	PGB	6.669871	14.16129	21.94868
Experiment 1	PGB	158.763	268.9754	228.5174
Experiment 1	PGB	37.80675	149.4193	259.2464
Experiment 1	PGB	54.92746	85.92131	100.3289
Experiment 2	PGB	16.98943	37.308	47.41
Experiment 2	PGB	0.785676	10.87868	20.37791
Experiment 2	PGB	6.104235	84.94565	141.4509

Experiment 2	PGB	2.541519	28.86793	54.86237
Experiment 2	PGB	8.245125	43.98406	89.10063
Experiment 3	PGB	24.76671	106.6281	135.1996
Experiment 3	PGB	0.68635	8.823325	14.73953
Experiment 3	PGB	14.1915	85.95713	241.7965
Experiment 3	PGB	3.700241	17.58548	38.77407
Experiment 3	PGB	93.6068	318.1882	705.3634
Experiment 4	PGB	14.33781	90.31062	170.2832
Experiment 4	PGB	3.556417	40.99992	117.5073
Experiment 4	PGB	31.42438	71.12178	149.7891
Experiment 4	PGB	17.65637	73.62221	159.6039
Experiment 4	PGB	17.1393	69.24617	156.1337
Experiment 1	TNF	7.348333	9.9442	32.352
Experiment 1	TNF	1.997895	7.333053	24.08068
Experiment 1	TNF	23.96	73.79467	135.4098
Experiment 1	TNF	3.8002	19.2788	64.6888
Experiment 1	TNF	41.11947	113.249	176.0015
Experiment 2	TNF	9.682042	12.46488	39.71477
Experiment 2	TNF	2.1694	13.79915	88.43595
Experiment 2	TNF	37.0365	162.7457	226.608
Experiment 2	TNF	51.21336	77.09271	88.58571
Experiment 2	TNF	34.77957	88.32071	112.7056
Experiment 3	TNF	16.87733	29.87756	40.15878
Experiment 3	TNF	16.34044	42.87	49.95267
Experiment 3	TNF	10.743	187.905	466.0718
Experiment 3	TNF	10.38132	42.90889	69.81779
Experiment 3	TNF	18.0267	107.0206	198.8508
Experiment 4	TNF	13.73932	83.32779	108.7564
Experiment 4	TNF	14.80514	49.53786	138.7503
Experiment 4	TNF	28.4016	53.9968	85.7202
Experiment 4	TNF	1.353429	27.972	196.9661
Experiment 4	TNF	9.226366	49.00222	96.10632

Well plate experiments data

CTR		Neurite length [µm]	Average neurite length / total cells [µm/cell]	Average neurite length / cells w neurites [µm/cell]	Proportion cells w neurites / total cells
experiment 1					
	12h	2262.92	20.39	377.15	0.11
	24h	7151.43	64.43	397.30	0.18
	36h	16385.85	147.62	321.29	0.46
experiment 2					
	12h	4506.24	51.21	643.75	0.06
	24h	8347.61	94.86	695.63	0.15
	36h	13190.18	149.89	573.49	0.26
experiment 3					
	12h	2847.52	30.29	203.39	0.12
	24h	6736.34	71.66	320.78	0.23
	36h	13638.88	145.09	247.98	0.59
experiment 4					
	12h	1195.55	8.66	91.97	0.09
	24h	4951.82	35.88	99.04	0.36
	36h	12179.71	88.26	154.17	0.57
PGB		Neurite length [µm]	Average neurite length / total cells [µm/cell]	Average neurite length / cells w neurites [µm/cell]	Proportion cells w neurites / total cells
experiment 1					
	12h	2595.21	38.16	370.74	0.11
	24h	6426.53	94.51	642.65	0.16
	36h	7643.94	112.41	449.64	0.25
experiment 2					
	12h	449.95	4.45	40.90	0.09
	24h	3558.29	35.23	169.44	0.17
	36h	6336.28	62.74	198.01	0.32

experiment 3					
	12h	981.64	10.12	89.24	0.09
	24h	4001.23	41.25	181.87	0.17
	36h	7480.83	77.12	173.97	0.43
experiment 4					
	12h	2522.09	19.86	86.97	0.23
	24h	9161.15	72.14	163.59	0.44
	36h	19545.50	153.90	205.74	0.75
TNF		Neurite length [µm]	Average neurite length / total cells [µm/cell]	Average neurite length / cells w neurites [µm/cell]	Proportion cells w neurites / total cells
experiment 1					
	12h	1028.98	15.36	114.33	0.14
	24h	2849.28	42.53	237.44	0.24
	36h	5394.19	80.51	245.19	0.33
experiment 2					
	12h	1690.79	17.80	140.90	0.08
	24h	3548.31	37.35	161.29	0.22
	36h	7063.82	74.36	164.27	0.45
experiment 3					
	12h	921.20	14.62	65.80	0.17
	24h	4737.84	75.20	278.70	0.23
	36h	8910.99	141.44	387.43	0.37
experiment 4					
	12h	1174.44	10.49	58.72	0.18
	24h	6379.71	56.96	155.60	0.37
	36h	13609.25	121.51	186.43	0.65

Devices experiments data

CTR	baseline 12h [µm]	endpoint 36h [µm]	% growth	difference total [µm]
experiment 1	39168.846	93633.491	239.0509309	54464.645
experiment 2	42547.169	133334.36	313.3800982	90787.191
experiment 3	47096.633	115921.004	246.1343765	68824.371
experiment 4	29828.855	81666.561	273.7837607	51837.706

PGB	baseline 12h [µm]	endpoint 36h [µm]	% growth	difference total [µm]
experiment 1	18036.161	69877.285	387.4288159	51841.124
experiment 2	91632.381	154448.297	168.552094	62815.916
experiment 3	84497.583	156991.315	185.7938528	72493.732
experiment 4	13179.687	57738.136	438.0842732	44558.449

TNF	baseline 12h [µm]	endpoint 36h [µm]	% growth	difference total [µm]
experiment 1	46757.735	115932.749	247.9434665	69175.014
experiment 2	65909.618	171413.659	260.0738165	105504.041
experiment 3	58576.63	140966.056	240.652383	82389.426
experiment 4	9015.759	43477.481	482.2387222	34461.722